Article

Implementation of Smart Tomographic Sensors in Cyber Physical System for Process Analysis in Industry 4.0

Tomasz Rymarczyk[1,2,*], Grzegorz Kłosowski[3], Edward Kozłowski[3], Paweł Tchórzewski[2]

[1] University of Economics and Innovation in Lublin, Poland; tomasz@rymarczyk.com
[2] Research & Development Centre Netrix S.A., Lublin, Poland
[3] Faculty of Management, Lublin University of Technology, Lublin, Poland; g.klosowski@pollub.pl, e.kozlovski@pollub.pl
[*] Correspondence: tomasz@rymarczyk.com

Abstract: The article presents a cyber-physical system for acquiring, processing and reconstructing images from measurement data. The technology was based on process tomography, intelligent measurement sensors, machine learning, Big Data, Cloud Computing, Internet of Things as a solution for Industry 4.0. Industrial tomography enables observation of physical and chemical phenomena without the need of internal penetration and allows real-time monitoring of production processes. The application includes specialized intelligent devices for tomographic measurements and dedicated algorithms for solving the inverse problem. The work focuses mainly on electrical tomography and image reconstruction using deterministic methods and machine learning, the reconstruction results were compared, different measurement models were used. The researches were carried out for synthetic data and laboratory measurements. The main advantage of the proposed system is the possibility of spatial data analysis and their high processing speed. The presented research results show that the process tomography gives the possibility to analyse the processes taking place inside the facility without disturbing the production, analysis and detection of obstacles, defects and various anomalies. Knowing the characteristics of a given solution, the application allows you to choose the appropriate method to reconstruct the image.

Keywords: inverse problem; industrial tomography; machine learning, sensors, cyber-physical system, Industry 4.0

1. Introduction

The article presents the results of research on the use of tomographic sensors for the analysis of industrial processes with the use of dedicated measuring devices, image reconstruction algorithms and the cyber-physical system (CPS). Advanced automation and control of production processes play a key role in enterprises. Technological equipment and production lines can be considered the heart of industrial production, while information technologies and control systems are its brain. They ensure high flexibility, fast adaptation of production processes to changing market requirements as well as safety and efficiency with optimal costs of resources and energy. The development and application of advanced mechanisms for process control ensures greater production flexibility.

Cyber-Physical Systems is a concept of systems with strictly integrated computational, physical and communication processes. In contrast to advanced systems, CPS create a unified structure for modelling and implementing complex systems as a whole. The presented concept of Cyber Intelligent Enterprise consists directly in the application of the CPS vision in the field of enterprise systems, the Internet of Things (IoT) and the semantic network. The tight integration of physical devices and business processes gives new possibilities and increases the efficiency of the enterprise [1]. Systems

Preprints (www.preprints.org) | NOT PEER-REVIEWED | Posted: 29 August 2018 doi:10.20944/preprints201808.0482.v1

of cooperating computing units that are in intense connection with the surrounding physical world and its current processes provide and use simultaneously data access and data access services available on the Internet. They can be part of the fourth industrial revolution, often labelled as Industry 4.0. Cyber-physical production systems (CPPS) are based on the latest developments in the fields of information technology, electronics, information and communication technologies. Such a solution consists of autonomous and cooperating elements and subsystems that connect with each other at all stages of production, from processes through machinery, to production networks and quality control. Autonomy, cooperation, optimization, integration of analytical approaches and simulations is related to the operation of sensor networks, large amounts of data and the search, analysis and interpretation of information with particular emphasis on security aspects [2]. The hybrid NC control system for an automatic line based on CPS technology uses a variety of techniques, such as sensors, intelligent computing and heterogeneous network integration [3]. Integration and intelligence are a development trend of production systems. Using the sensor network, it combines NC production line components, CNC production lines based on real-time information technology updates, intelligent control.

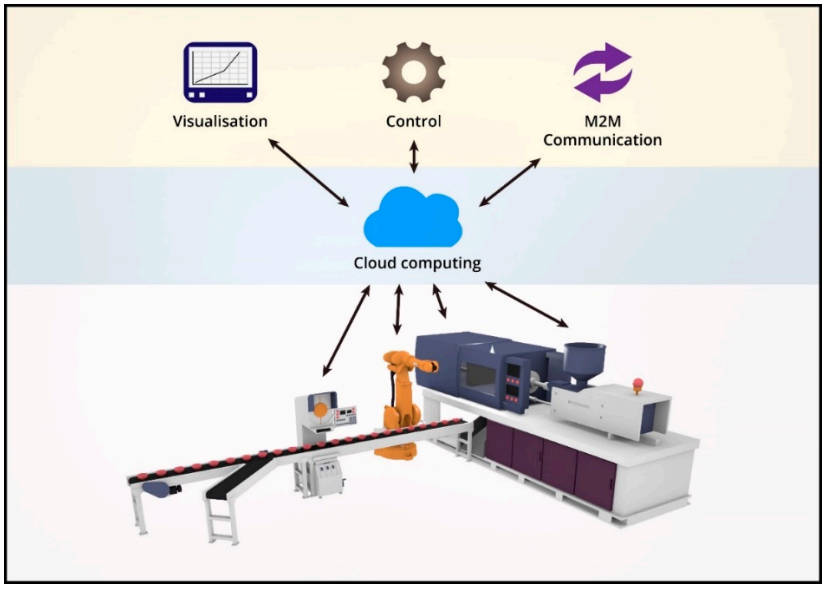

Figure 1. Industrial automation system based on a computing cloud

The implementation of a system combining real industrial environments with a virtual copy of components is presented in [4]. The system is based on virtual digital objects with a certain degree of complexity and autonomous control. IoT extends this concept with components of machine communication technology (M2M) and the ability to communicate and interact with physical objects represented by CPS. The system enables communication in the network and performing small tasks in a decentralized way autonomously, which contributes to the personalization of products and adapting the product's functions to local needs and their individual production process (Fig. 1). New technologies offer great opportunities to promote industrial modernization. They allow the introduction of the fourth industrial revolution. In the context of Industry 4.0, all kinds of smart devices supported by wired or wireless networks are commonly used (Fig. 2). Advances in the field of industrial Internet of Things (IIoT) and related fields such as industrial wireless networks (IWN), large data sets and cloud computing help create a new concept for industrial environments. Here one can pay attention to the architecture of the prototype platform deployment, the functions and features of each component layer, and the exchange of information between all types of devices [5]. Intelligent equipment and software are needed to build a smart factory. These include intelligent machine controllers, broadband devices, analytical systems for large data sets and integrated information applications. With the advent of new technologies (IoT, Cloud Computing, Big Data, Artificial Intelligence), intelligent machines and products can communicate with each other and negotiate for

Preprints (www.preprints.org) | NOT PEER-REVIEWED | Posted: 29 August 2018 doi:10.20944/preprints201808.0482.v1

reconfiguration in order to flexibly produce many types of products. Data can be collected from smart devices and transferred to the cloud. This gives feedback and coordination based on the analysis of large data to optimize system performance. Self-organized reconfiguration and communication based on a large amount of data determine the framework and operating mechanism of an intelligent factory in Industry 4.0 [6]. Intelligent production applications based on agents are an appropriate solution to the problem of production planning and scheduling, as production companies can include a variety of different elements, such as production process planning, monitoring and control. The agent-based implementation enables defining workflows and tracking production logic. In automation in production systems, multi-agent technologies can be used for parallel control, using cloud computing and service-oriented architecture (SOA) to share production resources [7].

Figure 2. The idea of the concept of Industry 4.0

Tomographic imaging of objects creates a unique opportunity to discover the complexity of the structure without the need to invade the object [8]. There is a growing need for information on how internal flows behave in the process equipment. It should be performed non-invasively by tomographic instrumentation. Conventional measuring instruments may either be unsuitable for difficult internal process conditions or their presence may interfere with the operation of the process. Process tomography is used to manipulate data from remote sensors to obtain precise quantitative information from inaccessible locations. It allows to improve the processes and their design, enabling real-time imaging of the boundaries between different components using non-invasive sensors. Information on substance properties, flow, vector velocity and concentration of ingredients in process vessels and pipelines can be determined based on the images obtained by installing sensors around the object to be imaged. Image data can be analysed online or collected for later use to run a process control strategy or to develop models describing particular processes. Online monitoring and diagnostics on the tomographic data streams can be incorporated into automated decision systems for industrial applications. Computer intelligence methods are capable of solving very complex tasks. Current tomographic systems provide limited support for computer intelligence methods, given the limited space and time of their embedded computational elements. The concept of distributed cloud computing architecture for online processing of tomographic data streams is presented in [9]. The monitored object is a tomographically instrumented part of the production plant, in which the tomographic device collects data by means of exciting electric potentials on its surface in a non-invasive way. The device sends raw data to the cloud computing system, where the inverse problem (image reconstruction) is solved. The final effect is the use of a machine learning algorithm to classify the status of the monitored object and make a specific decision by closing the control loop. Figure 1 shows the general scheme of the system operating in a closed loop.

Preprints (www.preprints.org) | NOT PEER-REVIEWED | Posted: 29 August 2018 doi:10.20944/preprints201808.0482.v1

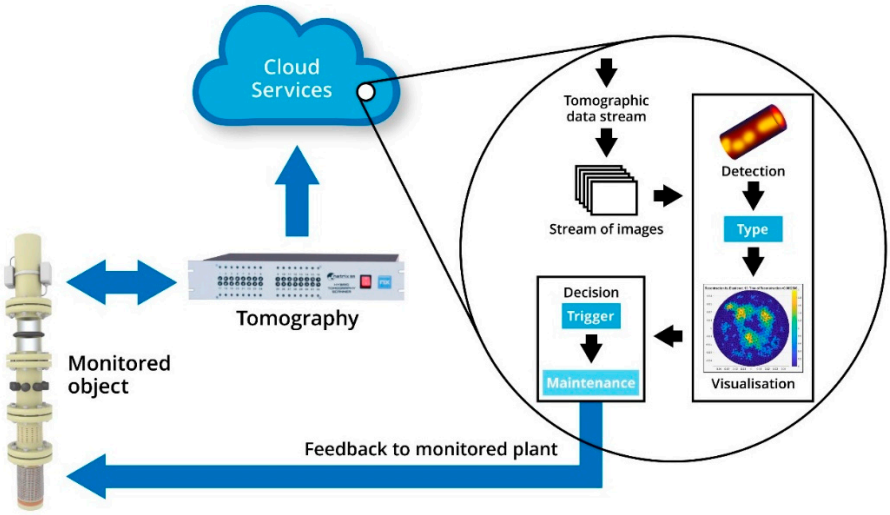

Figure 3. A general scheme of a system operating in a closed loop

Industrial tomography is a harmless, non-invasive imaging technique used in various industrial technologies to study physical and chemical processes without the need to penetrate their interior. It performs continuous data measurement, it allows better understanding and monitoring of industrial processes, enabling a quick response. This makes it easier to control processes in real time and incorrect system operations. The main advantage of tomographic examinations is their non-invasive nature, which does not cause changes that could interfere with the measurement results. Industrial tomography can be transformed into a powerful sensor solution for control. Distributed infrastructure requires various tasks related to the detection and start-up of processes, and is usually characterized by an internal spatial organization. The wireless sensor network (WSN) technology offers great opportunities in the aspect of cooperation of many devices in a wide range.

The presented solution enables the control of processes based on tomographic sensors, analysis of large data sets, multidimensional control of industrial processes, control using advanced human-machine interfaces and monitoring of knowledge-based processes. Sensor technologies are mainly based on electrical tomography (ET) [10-16], which includes capacitance tomography (ECT) [17-25] and resistance tomography (ERT) [26-28]. It allows reconstruction of the image by the distribution of conductivity or permittivity of the object from electrical measurements at the edge of the object. Another method is ultrasound tomography (UT) [29], which is a technique that uses information contained in the ultrasound signal after it passes through the examined object. However, by using a wire mesh sensor (WMS) a distribution of material properties in the gas and liquid flow is obtained in a direct manner. The project is implemented as part of research work at Research and Development Laboratory in Netrix S.A.

The article consists of 5 chapters. The architecture of the designed system with the industrial processes and the application platform is presented in Chapter 2. The methods and algorithms used to solve the inverse problem in image reconstruction, numerical models, tomographic devices and laboratory measurement systems are also described here. The results of research work in the form of reconstruction of images for synthetic and measurement data are shown in Chapter 3. In Chapter 4, the results obtained are discussed. Chapter 5 summarizes the research carried out.

2. Materials and Methods

This chapter presents the system model, tomographic methods, process tomography, measuring devices, laboratory systems, mathematical algorithms and measurement models used in image reconstruction based on synthetic data and real measurements. Laboratory equipment, tomography devices constructed at Research & Development Centre Netrix SA, the Eidors toolbox [30], Microsoft tools, Matlab, Python and R language were used for the research.

Preprints (www.preprints.org) | NOT PEER-REVIEWED | Posted: 29 August 2018 doi:10.20944/preprints201808.0482.v1

2.1. System architecture

Advanced control of production processes facilitates modelling of complex relations between process parameters, which guarantees stable, automated and flexible work. The main problem occurring in the research of technologically closed facilities is the lack of information allowing the analysis of the properties and quality of the substance being a component of the technological process. The presented technology allows for monitoring and acquisition of measurements at any time, which is useful for controlling the quality of production processes. Supervision and control take place within the scope of data obtained and processed as well as parameters of executive devices. It will allow to optimize the system in such a way that the processes themselves are always reproducible, leading to further increase of bandwidth, efficiency and quality of products.

The solution architecture consists of a cyber-physical system model, measurement sensors and methods for the analysis and classification of algorithms and image reconstruction. The system design was based on containers in the cloud computing model. The use of containers allows the use of public clouds. The use of a distributed system using microservices and containers allows the flexibility of a system in which modules perform clearly defined tasks. The modules are independent of each other, they can be easily replaced with newer versions, and the failure of one of the modules does not cause the whole system to fail. Such architecture will increase the reliability level of the new IT system. It will enable forecasting changes based on the analysis of historical data from the system as well as data obtained from devices in real time. An open platform model for a smart enterprise system (Fig. 4) contains measuring devices for acquiring sensor data, pre-processing and transmission to a system server network (Fig. 5). Another element of the solution is a portal which, together with data exchange interfaces (communication platform), enables management of data stored on the server and will contain documents and processes in the enterprise. Interfaces exchanging data with internal and external systems will participate in the process (Fig. 6). The algorithms of manual and automatic control relate to issues related to data processing, obtained from various sensors located in key nodes of the installation. The main feature of the use of wireless methods is the acquisition of the most important information about the process and installation status in real time by persons who are of strategic importance in the process of management and technical supervision. The transmitted data are analysed by an expert system and are used to optimize production processes (Fig. 7).

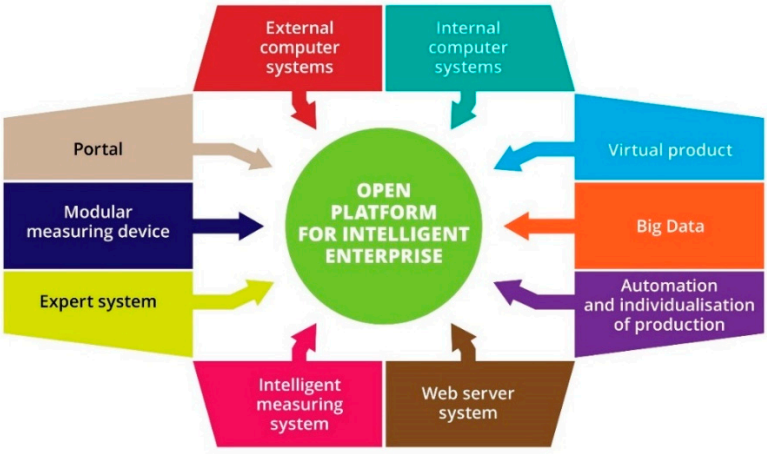

Figure 4. An open platform model for a smart enterprise system

Preprints (www.preprints.org) | NOT PEER-REVIEWED | Posted: 29 August 2018 doi:10.20944/preprints201808.0482.v1

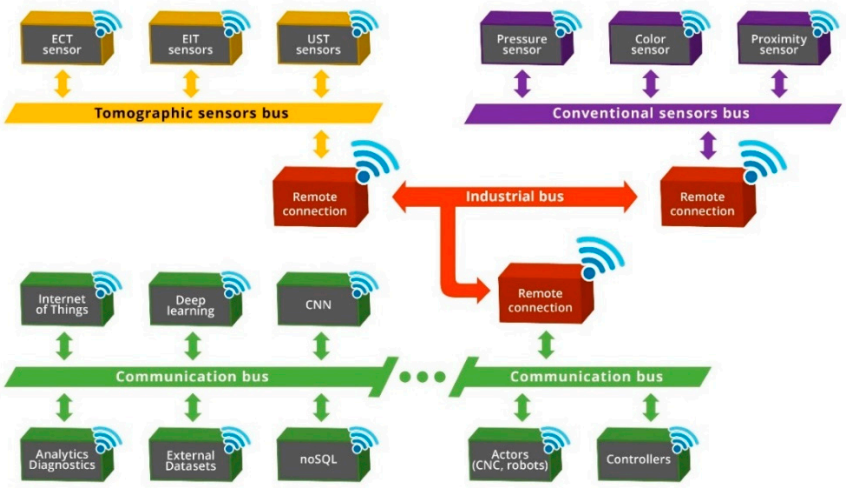

186

187 **Figure 5.** The communication model between the system elements

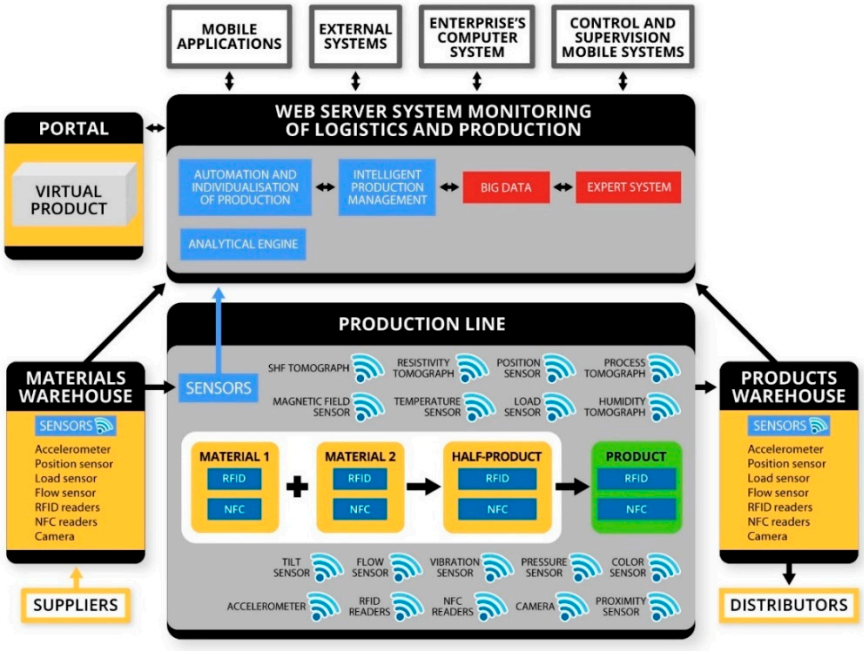

188

189 **Figure 6.** An intelligent system for the production and monitoring of processes

190

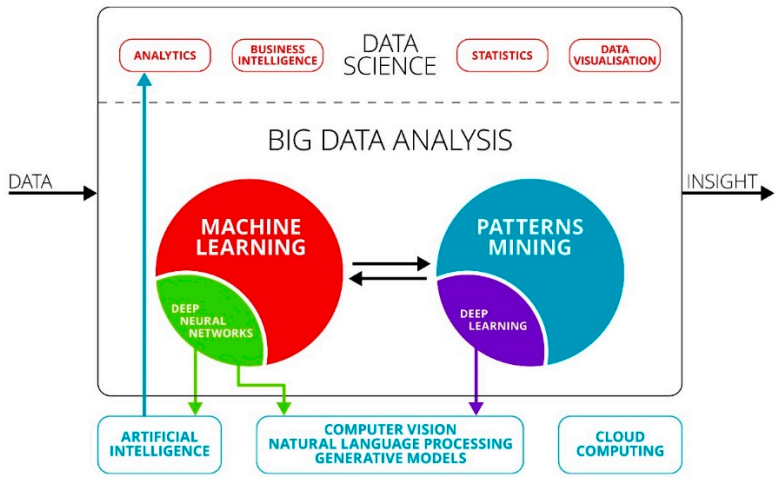

191

192 **Figure 7.** Analysis model of large data sets for machine learning

Preprints (www.preprints.org) | NOT PEER-REVIEWED | Posted: 29 August 2018 doi:10.20944/preprints201808.0482.v1

The central point of the system is a software integration platform that provides instruments for communication and management of smart devices. The platform consists of a communication layer, control software and multi-platform libraries and clients (Fig. 8).

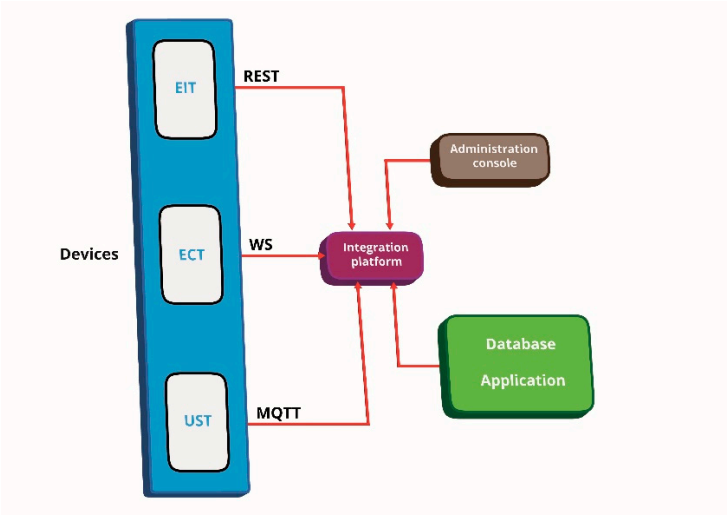

Figure 8. Block diagram of the integration platform of the system used to manage devices

From a technical point of view, the platform is scalable, based on microservices implemented on a local hardware platform with the main purpose to work on cloud platforms. The use of the integration platform provides support for the entire process related to device management and data processing. The process consists of stages. from data transfer, validation and collection to processing using algorithms. The integration platform can communicate with devices via the REST (Representational State Transfer) interfaces, the WebSocket (computer communications protocol), or the MQTT (Message Queuing Telemetry Transport) protocol. Almost all devices that support one of these protocols can be connected to the platform.

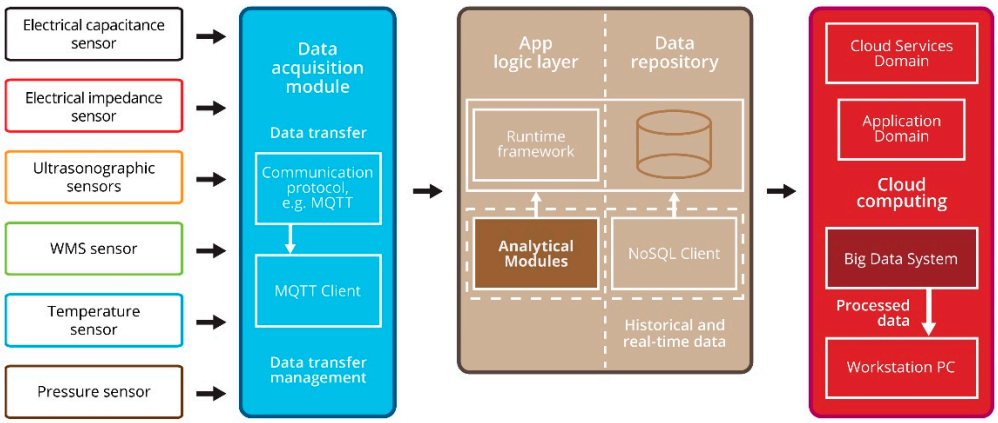

Figure 9. The structure model of the system for acquisition, processing, data collection and analysis in cloud computing

The structure model of the system for acquisition, processing, data collection and analysis in cloud computing was presented in Fig. 9. The data was collected from the devices. The MQTT protocol has been used to transfer data from the source to the analytical system. The data flow was repeated in two flows: the first was transmitted to the database system and the second was sent to the analytical system for further analysis. The purpose of this operation is to process data in real time and to store historical data for additional offline analysis.

Preprints (www.preprints.org) | NOT PEER-REVIEWED | Posted: 29 August 2018 doi:10.20944/preprints201808.0482.v1

218 *2.2. Electrical tomography*

219 Electrical tomography is an imaging technique that uses different electrical properties of
220 different types of materials, including biological tissues. In this method, the power or voltage source
221 is connected to the object, followed by the emergence of current flows or the distribution of voltage
222 at the edge of the object. The collected information is processed by an algorithm that reconstructs the
223 image. This tomography is characterized by a relatively low image resolution. Difficulties in
224 obtaining high resolution result mainly from a limited number of measurements, nonlinear current
225 flow through a given medium and too low sensitivity of measured voltages depending on changes
226 in conductivity inside the area. Electrical tomography has historically been divided into electrical
227 capacitive tomography, for systems dominated by dielectrics and electrical resistance tomography.
228 The basic theory can be obtained from Maxwell's equations.
229 A complex 'admittivity' can define as follows:

$$\gamma = \sigma + \mathrm{i}\omega\varepsilon \tag{1}$$

230 where ε is the permittivity, σ is the electrical conductivity, ω is the angular frequency.
231 In the case of the electric field strength (E), the current density (J) in the test area will be related to
232 Ohm's law:

$$J = \gamma E \tag{2}$$

233 The gradient of the potential distribution (u) has the form:

$$E = -\nabla u \tag{3}$$

234 Due to the fact that there are no sources from the Ampère law in the studied region, we have:

$$\nabla \cdot J = 0 \tag{4}$$

235 Potential distribution in a heterogeneous, isotropic area:

$$\nabla \cdot (\gamma \nabla u) = 0, \tag{5}$$

236 where u is the potential.
237 Where the capacitance or resistance dominates, the equation factor should be simplified to the form:

$$\nabla \cdot (\sigma \nabla u) = 0 \quad for \quad \frac{\omega\varepsilon}{\sigma} \ll 1 \quad \text{(ERT)} \tag{6}$$

$$\nabla \cdot (\varepsilon \nabla u) = 0 \quad for \quad \frac{\omega\varepsilon}{\sigma} \gg 1 \quad \text{(ECT)} \tag{7}$$

238 By solving the inverse problem, we obtain the distribution of material coefficients in the studied area.
239 Electrical resistance tomography in a process tomography can be interchangeably called electrical
240 impedance tomography (EIT). In the further part of the work, we will mainly use the name EIT [31-
241 35].
242 The opposite method and neighbouring method in EIT for collecting data from potential
243 measurements at the edge of an object for 16 electrodes was shown in Fig. 10.

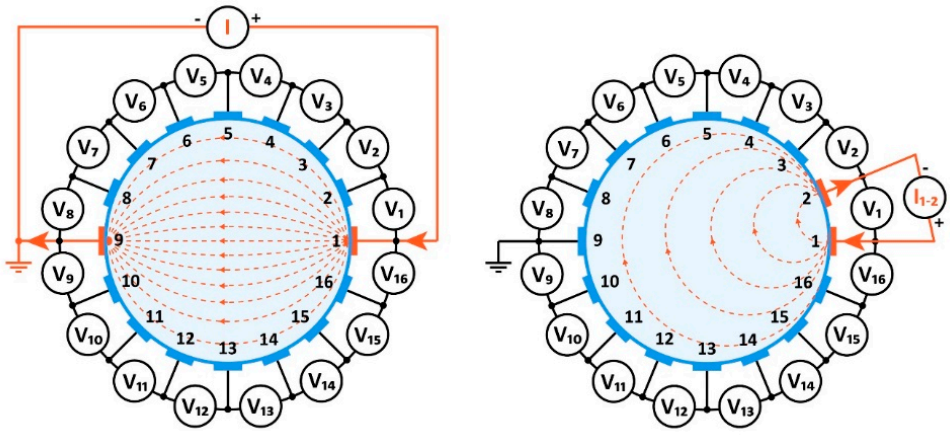

244
245 (a) (b)

246 **Figure 10.** Measurement model in electrical impedance tomography: (a) opposite, (b) neighbouring method

Preprints (www.preprints.org) | NOT PEER-REVIEWED | Posted: 29 August 2018 doi:10.20944/preprints201808.0482.v1

In electrical capacitive tomography, the source of information is the electrical capacity between the electrodes located on the edge of the object being tested (see Fig. 11). A very important feature of the measurement in the case of capacitive tomography is the lack of the need for physical interaction of the sensor with the medium being tested, thanks to which this method is non-invasive; that is, it does not disturb the ongoing industrial process. Another advantage of this measuring technique is the fast collection of measurement data. For measurements in capacitive process tomography, specially dedicated systems are used. Due to difficult measurement conditions, it is impossible to use ordinary capacitance measurements. Industrial processes run at high speed, so the measurement must be fast. In addition, the measured capacities are of the order of femtofarad, which requires special measuring techniques.

The inverse solution of the problem is achieved:

$$\varepsilon = S * C \tag{8}$$

where:

ε – permittivity matrix

C – capacity matrix

S – sensitivity matrix

Inverse problem can be solved with, for example using the Landweber algorithm:

$$\varepsilon_{k+1} = \varepsilon_k + \alpha * S^T * (S * \varepsilon_k - C_m) \tag{9}$$

where:

C_m- measured capacity matrix

ε_{k+1} – permittivity matrix, current iteration

ε_k – permittivity matrix, previous iteration

α – coefficient

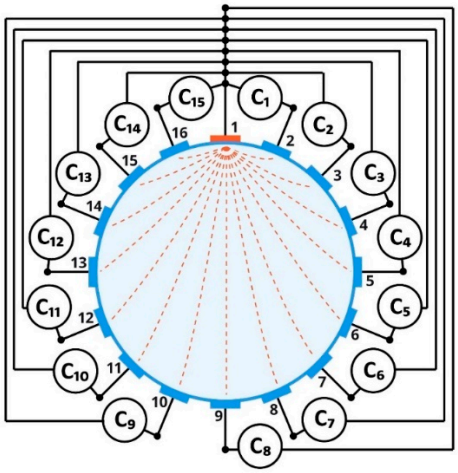

Figure 11. Measurement model in electrical capacitance tomography

2.3. Ultrasund tomography

Measurement methods using the information contained in the ultrasonic signal after passing through the tested medium are called ultrasound transmission methods. The main advantage of tomographic examinations is non-invasive measurement in the studied environment, which does not cause changes in physical and chemical parameters that could interfere with the measurement results. The measurement of parameters such as signal transition time, damping coefficient and its derivative by frequency enable, after appropriate reconstructive transformations, the imaging of the internal structure of the tested medium as well as such flow parameters as, for example: its instantaneous velocity, average speed or velocity profile. Differences in the local values of specific acoustic parameters are the basis of this imaging. The image obtained by appropriate reconstruction methods presents, because the distribution of local values of selected acoustic parameters obtained from measuring data by scanning technique from as many directions as possible after the ultrasonic pulses have passed through the tested environment. Ultrasonic transmission tomography for

Preprints (www.preprints.org) | NOT PEER-REVIEWED | Posted: 29 August 2018 doi:10.20944/preprints201808.0482.v1

detecting the two-component high-acoustic impedance mixture is used in chemical columns and industrial pipelines, where solid or gaseous particles inside liquid masses are repeatedly found [36]. The tomographic measurement data ensure control of various quality parameters of the material composition. A 2D transmission mode approach was used to reconstruct the acoustic velocity profile. According to the difference in the depth of penetration for given particle concentrations, the signal transit time has been calculated to detect a different material composition in the liquid mass.

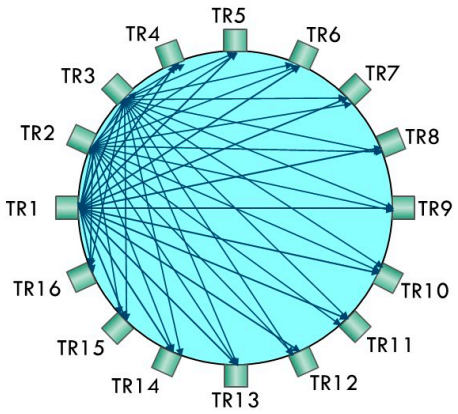

Figure 12. Sensor geometry for the ultrasonic tomography measurement system

The problem of image reconstruction in the case of ultrasounds leads to the equation in the form of a matrix:

$$W f = s, \tag{10}$$

where: s – right hand side vector (one column matrix), W is the matrix of dimensions m x n and m > n, f – the solution vector.

In order to solve the equation (10) is to find a vector f, which minimize Euclidean norm of residual vector r for the known matrix W and vector s, it means:

$$\|r\|_2 = min\|s - Wf\|_2, \qquad \|f^*\|_2 = min\|f\|_2 \tag{11}$$

where the last minimum is assumed for all vectors f that meet the previous relationship.

2.4. Wire mesh sensors

Wire Mesh Sensor is an invasive instrumentation measuring instantaneous phase distributions in two-phase flows (Fig. 13). WMS consists of two surfaces of wire electrodes; transmitters and receivers. The elements on each WMS plane are stretched parallel to each other and separated by a few millimetres and intersect each other at a 90 ° angle. The measurement of phase distributions is carried out at these intersection points, measuring electrical conductivity to conduct fluids or permeability of non-conductive fluids. On the basis of measurements of conductivity or electrical permeability, the amount of liquid and gas in single-volume components is calculated from the corresponding values [37].

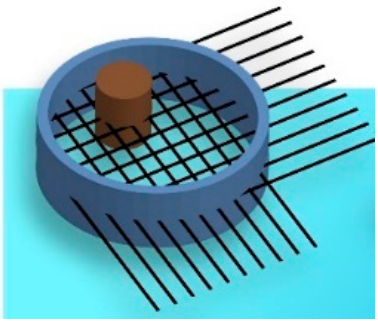

Figure 13. Model of wire mesh sensor

 doi:10.20944/preprints201808.0482.v1

2.5. Process tomography

Process tomography enables the analysis of processes taking place in the facility without interfering with them. It belongs to the opposite problems of the electromagnetic field; its purpose is to determine the properties of the tested object from measurements on its edge [38,39]. It enables better understanding and monitoring of industrial processes and facilitates process control in real time. The main difference in the mass production of chemicals, food and other commodities lies in the fact that common process sensors only provide local measurements. In production systems for the entire process, such local measurements are not representative, therefore spatial solutions are needed. Industrial processes are described in block models of energy and mass exchange elements. Process constituent units with often complex transfer functions derived from empirical process knowledge. The main difference is that a large number of parameter codes loses the spatial prediction capability and thus the current process conditions. In addition, their accuracy decreases, due to their inherent physical complexity in such phenomena as fluid dynamics, crystallization or fermentation process.

Data concentration profiles, phases and chemical substances can be investigated with fast data acquisition and image reconstruction. The obtained data can be used to monitor process reactions, improve quality, efficiency and flow rates. They can provide data for on-line process control. Typical industrial applications of process tomography are monitoring of varying concentration profiles in mixing and separation vessels (single-phase and multi-phase). Process tomography can allow you to control and understand processes in real time. It provides up-to-date feedback on processes, their effectiveness and progress in reactions. It can contribute to reducing waste and improving the overall energy efficiency of the company.

A change in reaction conditions can lead to a significant increase in production capacity, but it requires a significant change in many aspects of process design and unforeseen difficulties or benefits. The first element is to characterize the individual stages of the process. Process tomography sensors can provide quantitative and qualitative measurements of the dynamics and volume effects of the based processes. The data can be used as basic information about the process. The tomographic sensors can also help determine the efficiency of mixing and other performance characteristics. The tomography can be used to continuously monitor the effectiveness of the process by providing information when the reaction conditions change.

The installation of a two-phase flow identification system can be extremely useful in controlling the presence of air bubbles in liquids that are semi-finished products in which the presence of air is unacceptable. The existence of air bubbles in production processes can cause irreversible losses. Also, the presence of air in liquid semi-finished products with higher viscosities in the chemical, pharmaceutical and food industries can be very disadvantageous in some cases. Real-time control to detect the presence of air bubbles.

Crystallization is a key reaction in the pharmaceutical sector and other processes. The combination of two ionic species in solution to form a solid part often results in a strong change in electrical properties. The tomographic sensors can study the entire area and provide information on reaction kinetics and concentrations. This can help you pinpoint the reaction endpoints more accurately, as well as provide information on how to ensure the right chemical conditions. The tomographic measurements can also be used in various process ranges to confirm the scale characteristics. Crystallization is a widespread industrial process for the purification of substances and the conversion of dissolved compounds into solid products.

Figures 15 and 16 present measurement models for process tomography based on electrical and ultrasonic tomography. Figure 14 presents the idea of system structure with a hybrid tomography scanner with flow measurement, image processing in the cloud computing. The model of analysing the process of crystallization and fermentation is presented in Fig. 17. The UST is more suitable for detecting connections between materials, while ECT better characterizes individual phases. ERT is used to visualize the concentration profile.

Preprints (www.preprints.org) | NOT PEER-REVIEWED | Posted: 29 August 2018 doi:10.20944/preprints201808.0482.v1

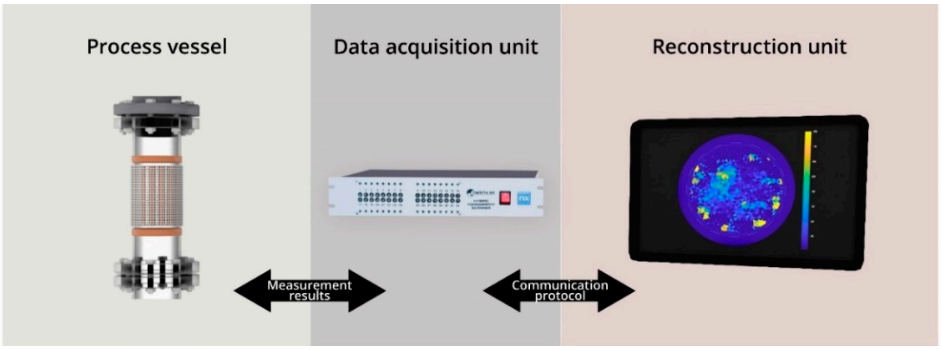

361

362 **Figure 15.** Measurement model for electrical tomography

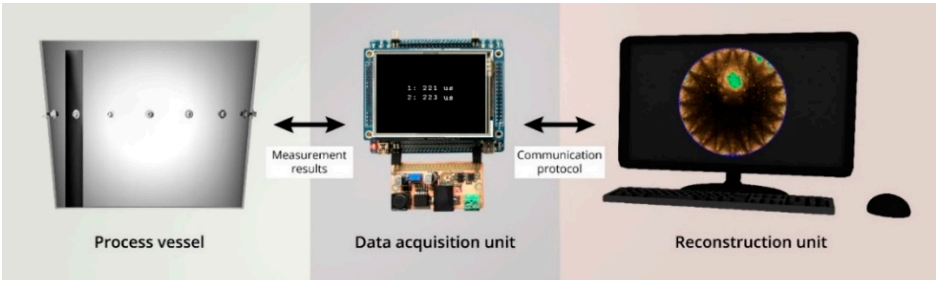

363

364 **Figure 16.** Measurement model for ultrasound tomography

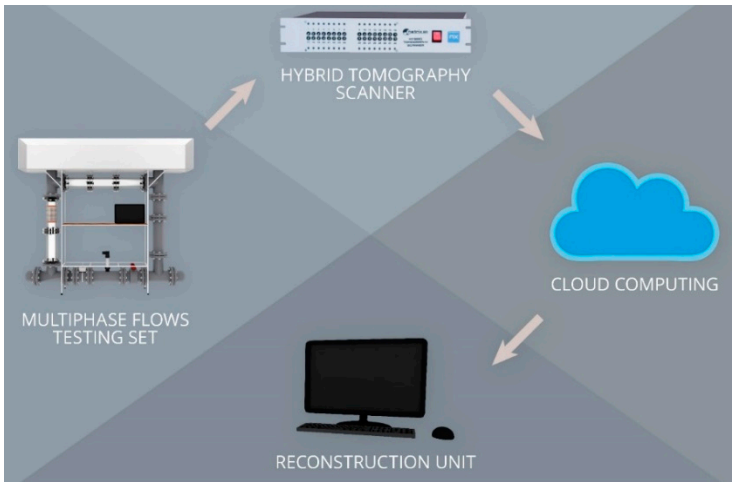

365

366 **Figure 14.** The idea of system structure with a hybrid tomography scanner with flow measurement, image
367 processing in the cloud computing

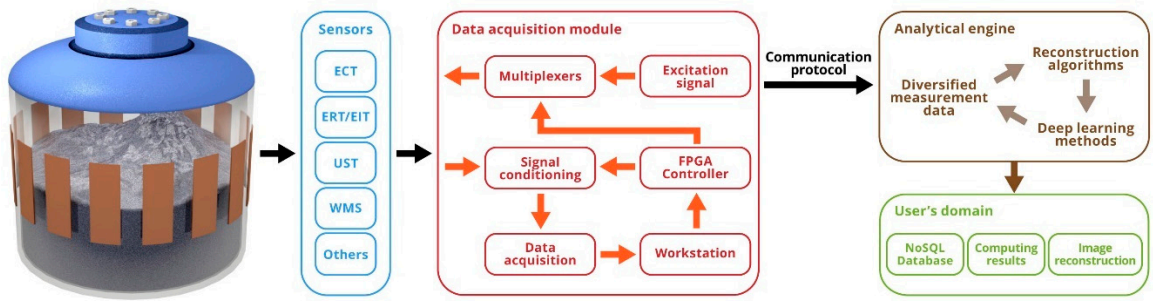

368

369 **Figure 17.** Monitoring, analysis and control processes in the test tank by tomographic methods

370

371

Preprints (www.preprints.org) | NOT PEER-REVIEWED | Posted: 29 August 2018 doi:10.20944/preprints201808.0482.v1

372 *2.6 Measurements systems*

373 *2.6.1. System model*

374 The idea of a measuring system is based on tomographic sensors. The appropriate types of
375 electrodes are placed on the measuring object (Fig. 18). Data acquisition module collects data and
376 through appropriate communication protocols send them to cloud computing, where they are used
377 in tomographic processes.

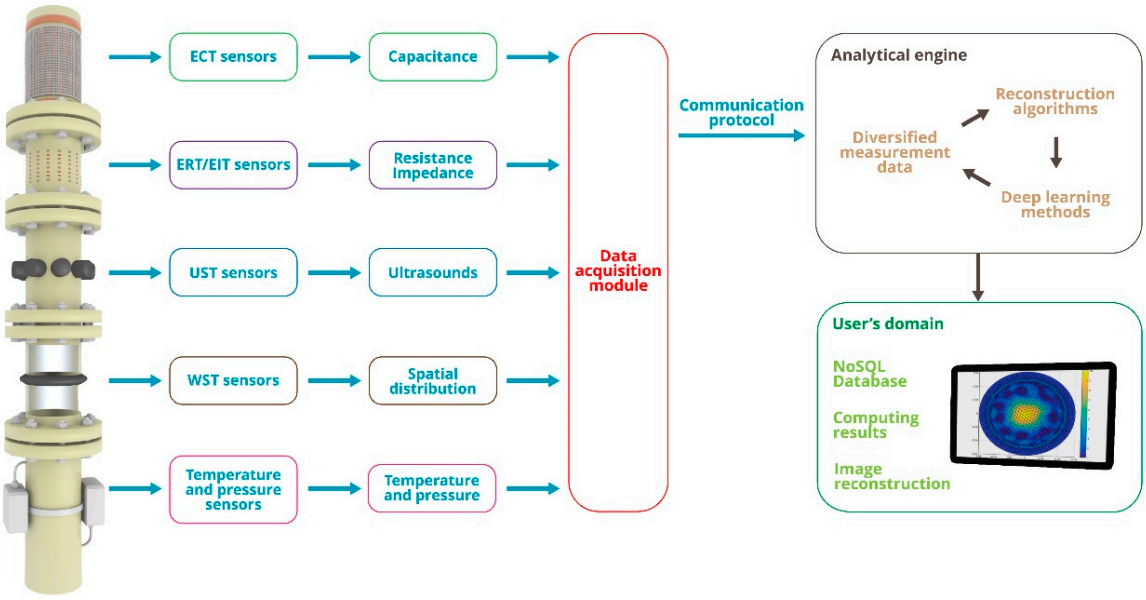

378

379 **Figure 18.** The idea of a measurement and analytical system

380 *2.6.2. Hybrid tomography scanner*

381 The construction of a hybrid tomography scanner was based on an electrical tomography and
382 measures the tested object based on measurements of potential distribution or capacitance. The
383 system collects the measured data from the electrodes. The device provides a non-invasive method
384 of testing the spatial distribution of material coefficients. Presented device for electrical tomography
385 includes two measuring methods using 32 channels. The measurements are based on electrical
386 capacitance tomography and electrical impedance tomography. The device is presented in Figure 19
387 in the form: measuring block, control and communication system, view from the inside and
388 measuring panel.

389

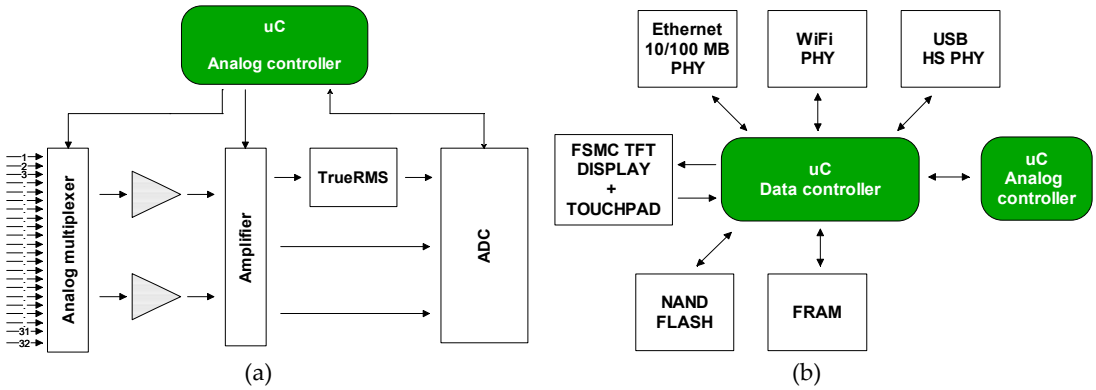

390
391

Preprints (www.preprints.org) | NOT PEER-REVIEWED | Posted: 29 August 2018 doi:10.20944/preprints201808.0482.v1

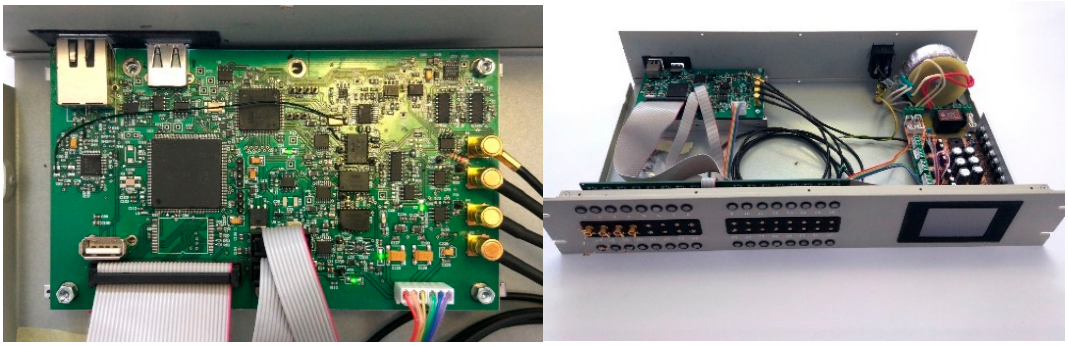

(c) (d)

Figure 19. Hybrid tomography scanner: (a) measuring block, (b) control and communication system, (c) view from the inside, (d) measuring panel

2.6.3. Ultrasound tomography system

The ultrasonic tomograph consists of active measuring probes controlled by an external module via a CAN bus. Active measuring probes are divided into digital and analog parts. The digital part is responsible for sending ready measurement results to the tomography controller via the bus. The analog part has been adapted to work with a piezoelectric transducer operating at 48 kHz. The active probe can work both as a receiver of an ultrasonic signal and as a transmitter. The main CT controller is responsible for managing the sequence of measurements, setting up active probes in the transmit / receive mode, and recording results taken from other probes. The probes are designed so that they can be placed very close to each other. Power lines, communication buses and interrupt lines necessary for correct timekeeping from the moment of sending to receiving the signal on other probes were carried out using RJ-12 cables. Figure 20 shows ultrasound tomography device: block diagram, model of measuring probe, start-up control module and active measuring probe.

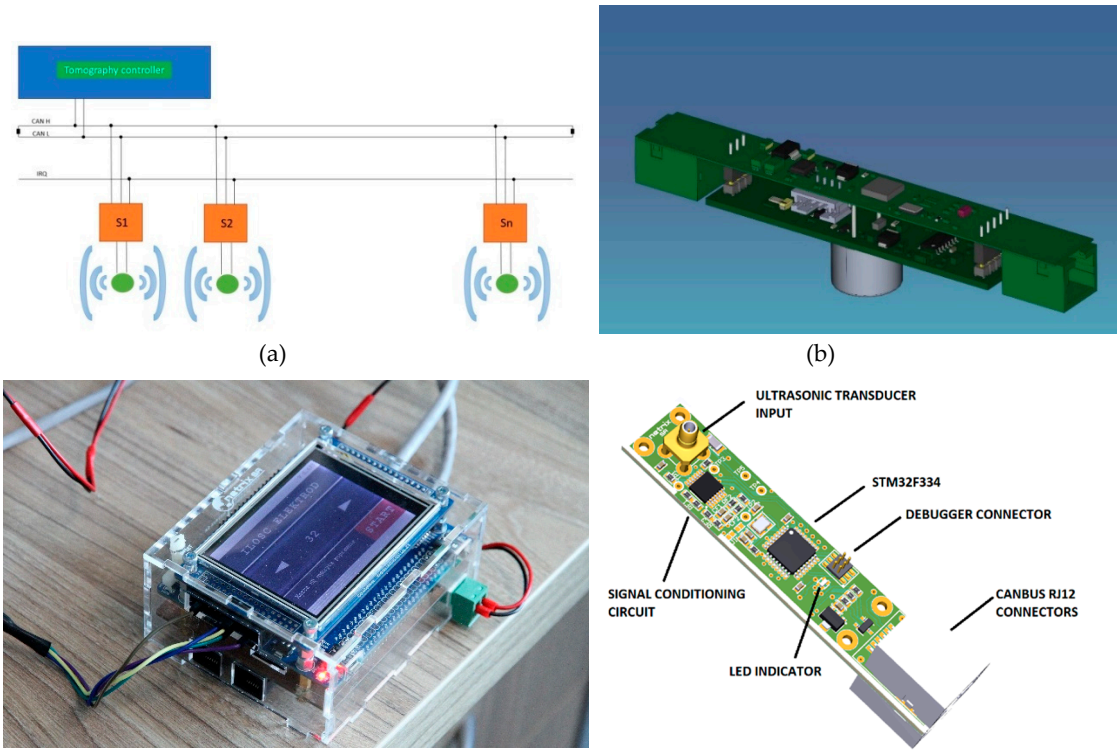

(a) (b)

(c) (d)

Figure 20. Ultrasound tomography device: (a) block diagram, (b) model of measuring probe, (c) start-up control module, (d) active measuring probe

Preprints (www.preprints.org) | NOT PEER-REVIEWED | Posted: 29 August 2018 doi:10.20944/preprints201808.0482.v1

2.6.4. Wire mesh sensor system

Wire mesh sensors are flow imaging devices and enable testing of multiphase flows with high spatial and temporal resolution. Although they could not be considered to belong to the classic tomographic technique because their operating principle relies on unwanted electrodes to generate images, it was considered an alternative technique of previously described tomographic systems. The sensor is a hybrid device between undesirable local measurement of phase fractions and a tomographic cross-section image. The sensor consists of two sets of wires extending in the cross-section of a tank or pipe with a small axial distance between them. Each plane of parallel wires is located perpendicular to each other to form a grid of electrodes. The associated electronics measure the local conductivity in the gaps of all transitions exceeding a high degree of repetition. Considering the two-phase flow, it consisted of an electrically conductive phase and the other non-conductive phase, for example air and water, the obtained conductivity measurements are indications of the phase present at each intersection point. The sensor is able to determine the instantaneous distribution of free fractions in the cross-section. Regarding the principle of measurement, a multiplexer pattern of excitation is used. The wires of one plane are used as transmitters, and the wires of the other plane as receivers. Figure 21 is a block diagram of the electronics of the conductivity grid sensor for an exemplary sensor configuration. Samples from all take-up lines are taken at the same time. This procedure is repeated for all transducer electrodes. The measurements are actually voltages that are proportional to the conductivity of the medium around each intersection of the wire mesh at the time of data extraction. In this way, the grid divides the cross section of the flow channel into several independent subregions, where each intersection constitutes one subregion. Each of the measured signals reflects the flow component in the associated subregion, i.e. each intersection operates as an indicator of the local phase. Thus, the set of data obtained from the sensor directly represents the phase distribution in the cross-section.

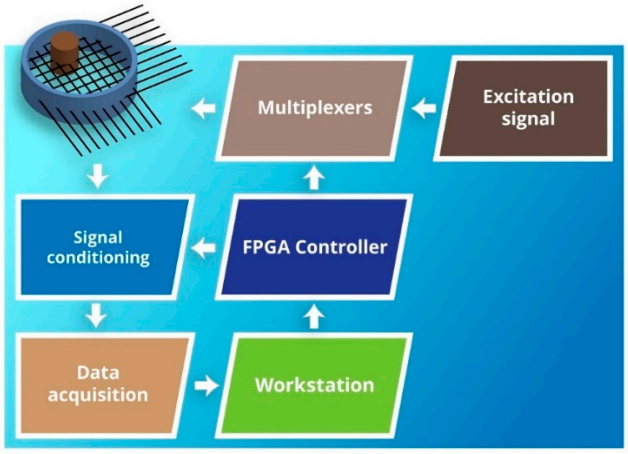

Figure 21. System model of wire mesh sensor

2.7. Laboratory models

In the Research and Development Centre of Netrix S.A. measuring stations for liquid flows (Fig. 22), the positions for tanks for electrical impedance tomography (Fig. 23) and ultrasound tomography (Fig. 24) were prepared. In this position, the sets of electrodes were placed on the examined objects. Sample image reconstructions made using the ultrasound tomograph are shown in Fig. 25.

Preprints (www.preprints.org) | NOT PEER-REVIEWED | Posted: 29 August 2018 doi:10.20944/preprints201808.0482.v1

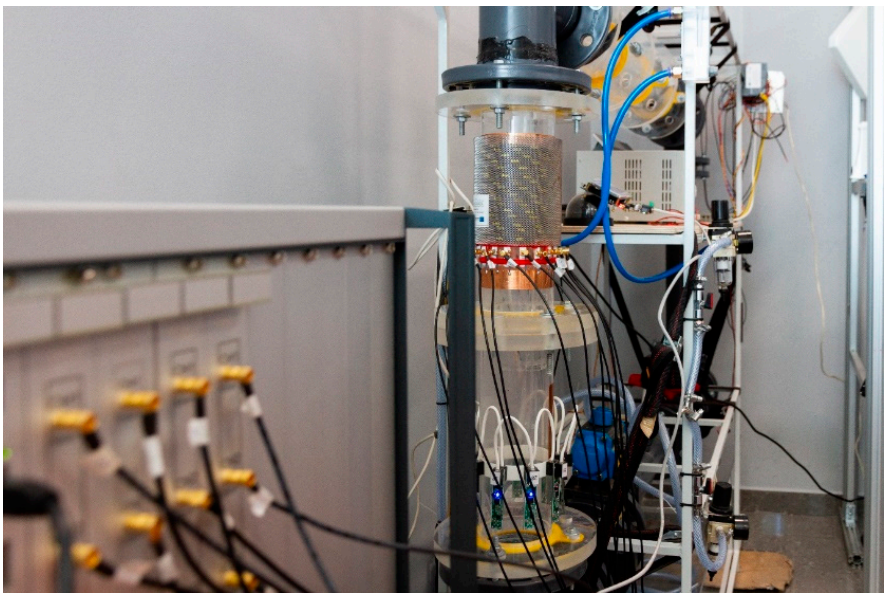

(a)

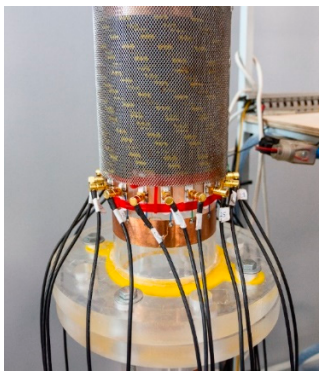

(b)

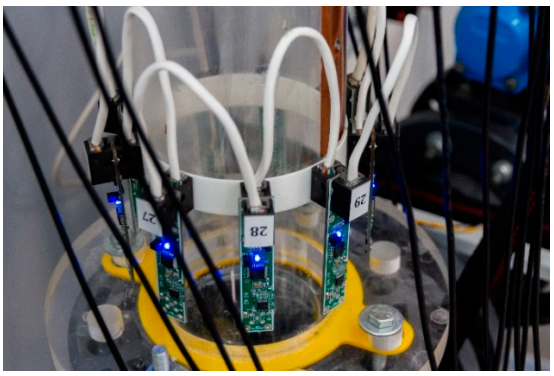

(c)

Figure 22. Laboratory model for liquid flows: (a) measuring system, (b) ECT probe, (c) UST probe

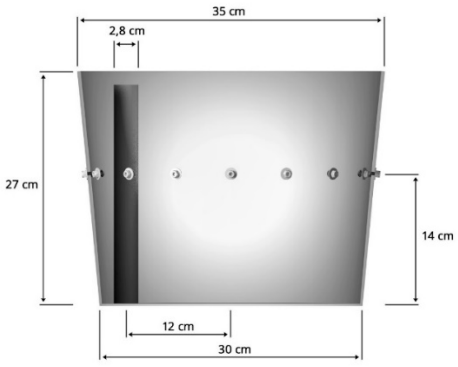

(a)

(b)

Figure 23. Model of the EIT measurement tank: (a) dimensions, (a) a bucket with electrodes

Preprints (www.preprints.org) | NOT PEER-REVIEWED | Posted: 29 August 2018 doi:10.20944/preprints201808.0482.v1

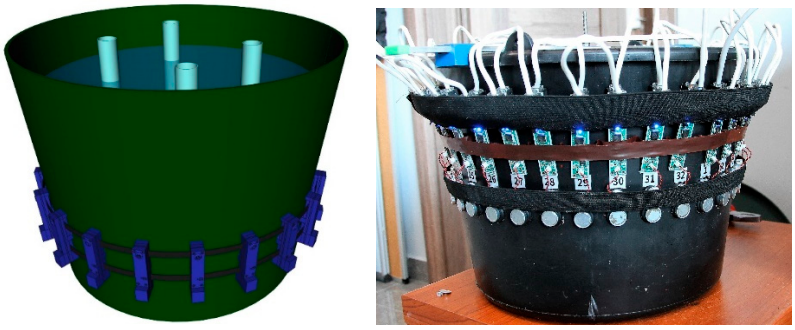

(b) (b)

Figure 24. The UST measuring tank: (a) model, (a) real object with the active electrodes

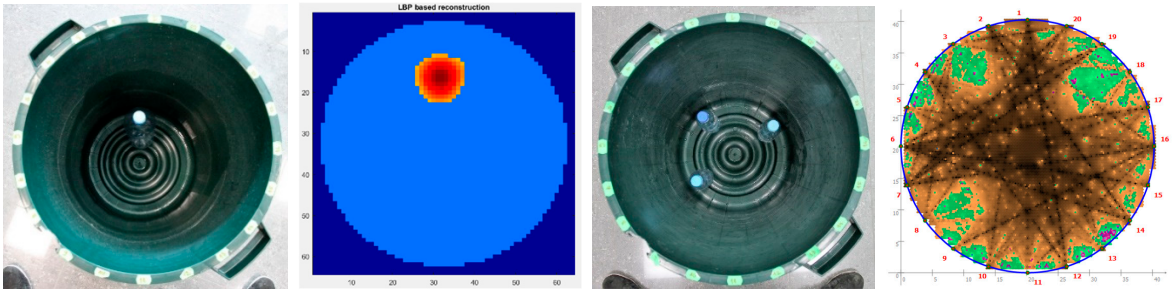

(c) (b) (c) (d)

Figure 25. Examples of reconstruction using UST for 20 measuring points with 48 kHz transducers: (a) 1 phantom, (a) image reconstruction for 1 object, (a) 3 phantoms, (a) image reconstruction for 3 objects

2.8. Measurement models

In order to test the effectiveness of algorithms for the analysis of processes in industrial tomography, three measuring models were selected. Electrical tomography was used for the analysis. The arrangement of phantoms inside the object under test were presented in Fig. 26. The measuring tank is shown in Fig 27.

(a) (b) (c)

Figure 26. The arrangement of phantoms inside the object under test: (a) 2 phantoms, (a) 3 phantoms, (a) 4 phantoms

Preprints (www.preprints.org) | NOT PEER-REVIEWED | Posted: 29 August 2018 doi:10.20944/preprints201808.0482.v1

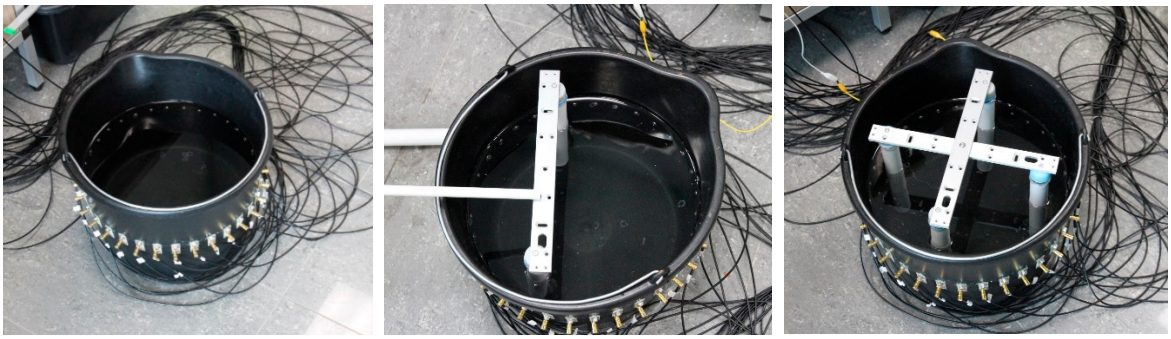

(a) (b) (c)

Figure 27. Measuring tank: (a) bucket with electrodes, (a) 2 phantoms, (a) 4 phantoms

2.9. Numerical models

An important element in the process of testing the effectiveness of algorithms is the preparation of numerical models. They were prepared in two variants: for 16 and 32 electrodes (Fig. 28 and Fig. 29).

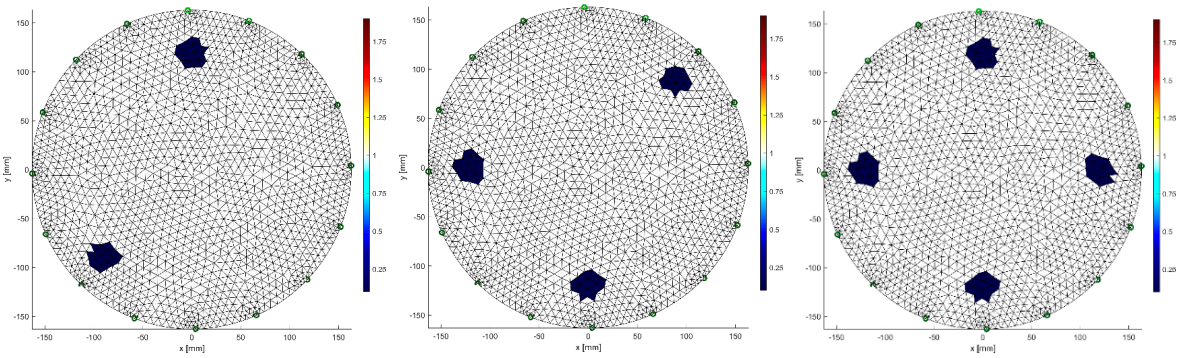

(a) (b) (c)

Figure 28. Numerical models for 16 measuring electrodes: (a) 2 objects, (b) 3 objects, (c) 4 objects

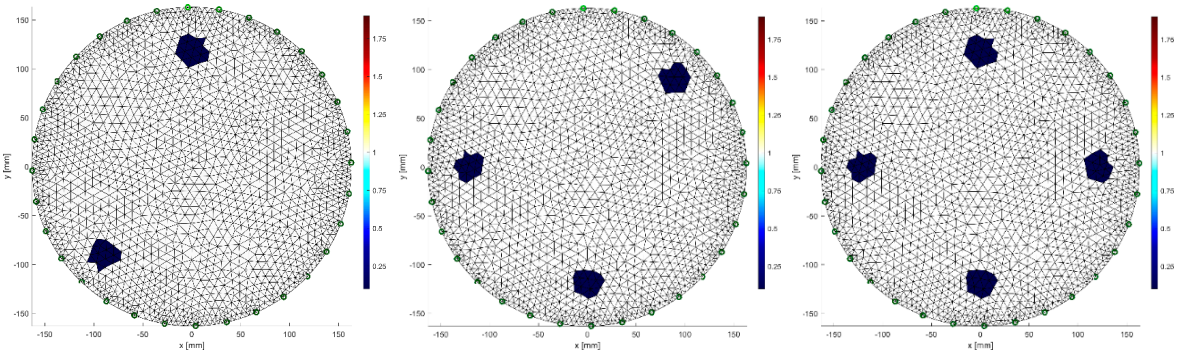

(a) (b) (c)

Figure 29. Numerical models for 32 measurement electrodes: (a) 2 objects, (b) 3 objects, (c) 4 objects

2.10. Algoruthms and methods

There are many methods and algorithms used in optimization problems [40-51]. In this article, the authors chose deterministic algorithms based on the Gauss-Newton and Total Variation methods, often used and quite effective in electrical tomography. The next algorithms were based on machine learning method [52-56]s, in which an innovative approach to tomographic problems was presented.

Preprints (www.preprints.org) | NOT PEER-REVIEWED | Posted: 29 August 2018 doi:10.20944/preprints201808.0482.v1

494 *2.10.1. Image reconstruction*

495 Process tomography also belongs to the problems of the inverse electromagnetic field. The
496 inverse problem is the process of optimization, identification, or synthesis in which the parameters
497 describing a given field are determined based on the possession of information specific to this field.
498 Such issues are difficult to analyse. They do not have unambiguous solutions and are ill-conditioned
499 due to too little or too much information. They are sometimes contradictory or linearly dependent.
500 Knowledge of the process can make image reconstruction more resistant to incomplete or damaged
501 data. The numerical analysis of the problem was carried out using the finite element method.

502 *2.10.2. Gauss-Newton method*

503 The Gauss-Newton Method is a very effective method. It is based on the first derivatives of the
504 vector function components implemented. In special cases, it may give a square convergence [57].
505 Electrical tomography is a nonlinear problem, and it has an inverse ill-posed problem. Gauss-Newton
506 algorithm can use to minimize differences between homogeneous and heterogeneous data [58].
507 Image reconstruction involves determining the global minimum of the objective function, which can
508 be defined as follows:

$$F(\sigma) = \frac{1}{2}\left\{ \left\| L_1 \left(U_m - U_s(\sigma)\right)\right\|^2 + \lambda^2 \left\| L_2 \left(\sigma - \sigma^*\right)\right\|^2 \right\}, \quad (12)$$

509 where:
510 Um - voltages obtained as a result of the measurements,
511 Us(σ) - voltages received by numerical calculations (FEM),
512 σ - conductivity,
513 σ* - conductivity represents known properties,
514 λ - regularization parameter - positive real number,
515 L1 - some square matrix,
516 L2 - regularization matrix.
517 Using appropriate approximations, it can be shown that the conductivity proper in the iteration
518 denoted by k + 1 is given by the following formula:

$$\sigma_{k+1} = \sigma_k + \alpha_k \left(J_k^T W_1 J_k + \lambda^2 W_2\right)^{-1} \left[J_k^T W_1 \left(U_m - U_s(\sigma_k)\right) - \lambda^2 W_2 \left(\sigma_k - \sigma^*\right)\right], \quad (13)$$

519 where: W1 - weighting matrix - it is usually a unit matrix, Jk - Jacobian matrix calculated in k-th step,
520 αk - step length.

521 *2.10.3. Total Variation*

522 In machine learning and inverse problems, regularization provides additional information to
523 solve the problem. Representative information is considered by introducing a penalty function based
524 on constraints for a given solution or boundaries in the vector space standard. Certain cases of
525 statistical regularization include methods such as dorsal regression, lasso and L2 norm. The concept
526 of regularization is based on the application of standards. Total Variation (TV) regularization is a
527 deterministic technique that protects discontinuities [59]. The Total Variation algorithm is used to
528 maintain the discontinuity value on the resulting reconstruction, so that the obtained images have
529 sharp edges at the discontinuity.
530 The objective function can be defined as follows:

$$F(\sigma) = \frac{1}{2} \| U_s(\sigma) - U_m \|^2 + \lambda \sum_{k=1}^{N} | R_k \, \sigma |, \quad (14)$$

531 where:
532 λ - regularization parameter,
533 Ri - a row vector that represents a discrete approximation of the gradient operator,
534 N - number of finite element mesh edges.
535

Preprints (www.preprints.org) | NOT PEER-REVIEWED | Posted: 29 August 2018 doi:10.20944/preprints201808.0482.v1

2.10.4. Lars

Machine learning is related to the ability of the software to generalize based on previous experience. The important thing is that these generalizations are designed to answer questions about both previously collected data and new information. Using statistical methods with different regression models were presented in [60]. This approach enables quick diagnosis combining low cost and high efficiency. The selection of variables and the detection of data anomalies are not separate problems. To use the variables and outliers at the same time, the low angle regression (LARS) algorithm is used. While it is prudent to be cautious about the generalization of a small set of simulation results, it seems that LARS combined with dummy variables or row samples can provide computationally efficient, robust selection procedures [61]. The proposed LARS algorithm calculates all possible Lasso estimates for a given problem using an order of magnitude of less computing time. Another variation of LARS implements the linear regression of Forward Stagewise, this combination explains similar numerical results previously observed for Lasso and Stagewise and helps to understand the properties of both methods. A simple approximation of LARS degrees of freedom is available, from which the estimated prediction error value [62] is taken.
If the regression data has only additional outliers, then we can start with a simple regression model:

$$Y = X\beta + \varepsilon, \tag{15}$$

where $Y \in R^n, X \in R^{n\times(k+1)}$ denote the observation matrices of response and input variables respectively, $\beta \in R^{k+1}$ denotes the vector of unknown parameters. The object $\varepsilon \in R^n$ presents a sequence of disturbances. Least Angle Regression algorithm includes to linear model only causal variables should be included. The linear model is built by employing the forward stepwise regression, where at each step the best variable is inserted to model.
Algorithm of Least Angle Regression is following:

- the predictors should be standardized,
- calculate the residuals,
- move coefficient β towards its least-squares coefficient.

Repeat until all predictors have been entered.

2.10.5. Elastic net

Elastic net is a regularized regression method that linearly combines the L1 and L2 penalties of the Lasso and ridge methods [63-66]. Lasso is a regularization technique. This method can be used to reduce the number of predictors in a regression model or it selects among redundant predictors.
The equation is used to determine the linear regression:

$$\min_{(\beta_0,\beta')\in R^{k+1}} \frac{1}{2n}\sum_{i=1}^{n}(y_i - \beta_0 - x_i\beta')^2 + \lambda P_\alpha(\beta'), \tag{16}$$

where $x_i = (x_{i1}, \dots, x_{ik}), \beta' = (\beta_1, \dots, \beta_k)$ for $1 \le i \le n$ and P_α is an elastic net penalty
P_α is defined as:

$$P_\alpha(\beta') = (1-\alpha)\frac{1}{2}\|\beta'\|_{L_2} + \alpha\|\beta'\|_{L_1} = \sum_{j=1}^{k}\left(\frac{1-\alpha}{2}\beta_j^2 + \alpha|\beta_j|\right), \tag{17}$$

We see that the punishment is a linear combination of norms L_1 and L_2 of unknown parametersβ'. The introduction of the parameter-dependent penalty function to the objective function reduces the estimators of unknown parameters.

2.10.6. Neural Network

This chapter presents the neuronal model enabling efficient reconstruction of tomographic images. Effective use of artificial neural networks in tomography is possible, but the effectiveness of this tool depends on many conditions. First of all, ANN (artificial neural networks) are able to effectively visualize objects, many of which are already known. A characteristic feature that distinguishes the discussed model is the separate training of neural networks in the amount equal to

Preprints (www.preprints.org) | NOT PEER-REVIEWED | Posted: 29 August 2018 doi:10.20944/preprints201808.0482.v1

the resolution of the output image grid. A suitable model of a neural tomographic system is shown in Fig. 30.

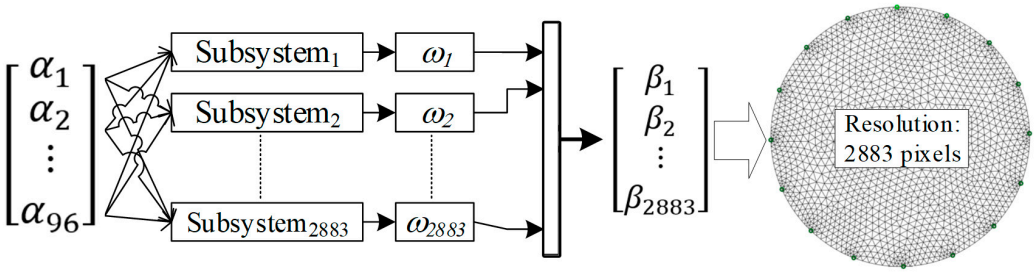

Figure 30. A mathematical neural model for converting electrical signals into images

3. Results

This chapter presents the results of image reconstruction based on built numerical models and laboratory measurements. Data analysis is an important part of the diagnosis of the process based on tomography. Knowledge of the process can make the image reconstruction better. Inside the area, a mesh of finite elements is generated. As a result of the calculations it obtains a reconstructed image. The inverse problem was solved using deterministic methods and machine learning.

3.1. Image reconfiguration for syntetic data

3.1.1. Gauss-Newton method

The Gauss-Newton method in two variants was used to reconstruct the image in the electrical tomography for the 16 and 32 electrode systems. The first model includes Laplace regularization (Figures 31 and 32), while the second variant has Tikhonov regularization (Figures 33 and 34). Reconstructed objects show models with 2, 3 and 4 inclusions.

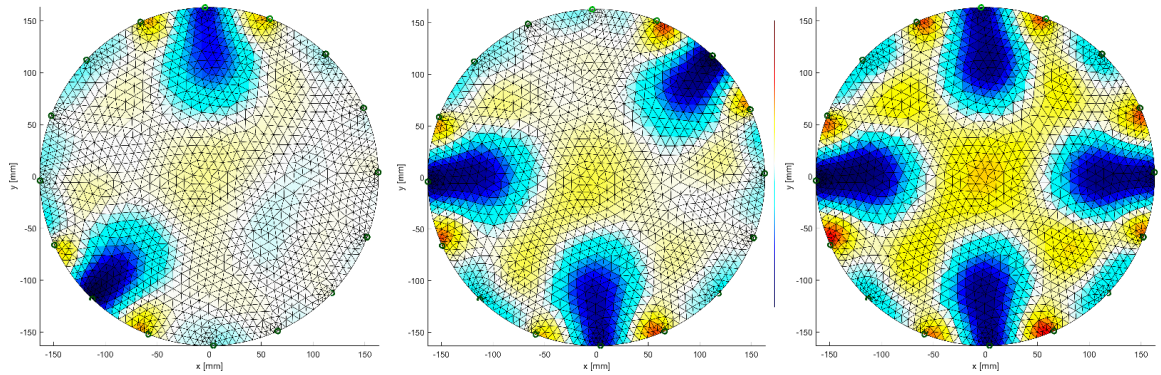

(a) (b) (c)

Figure 31. Image reconstruction for 16 measurement electrodes by Gauss-Newton method with Laplace regularization: (a) 2 objects, (b) 3 objects, (c) 4 objects

Preprints (www.preprints.org) | NOT PEER-REVIEWED | Posted: 29 August 2018 doi:10.20944/preprints201808.0482.v1

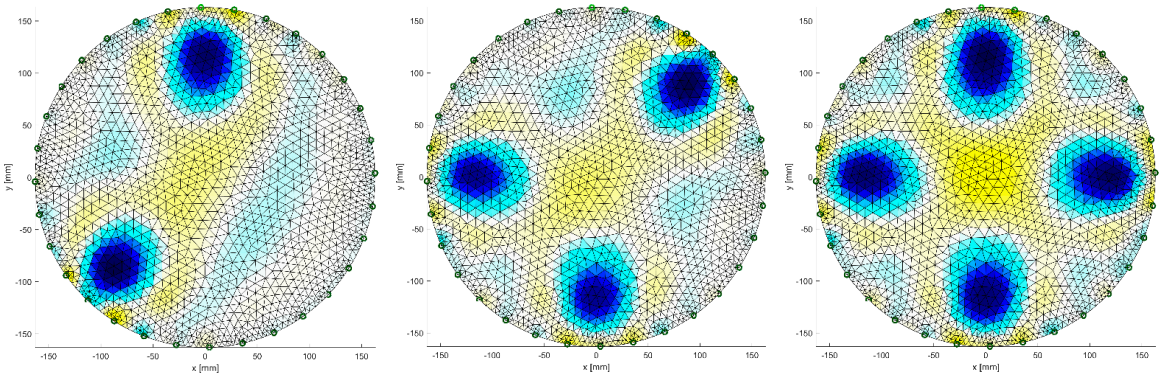

(a) (b) (c)

Figure 32. Image reconstruction for 32 measurement electrodes by Gauss-Newton method with Laplace regularization: (a) 2 objects, (b) 3 objects, (c) 4 objects

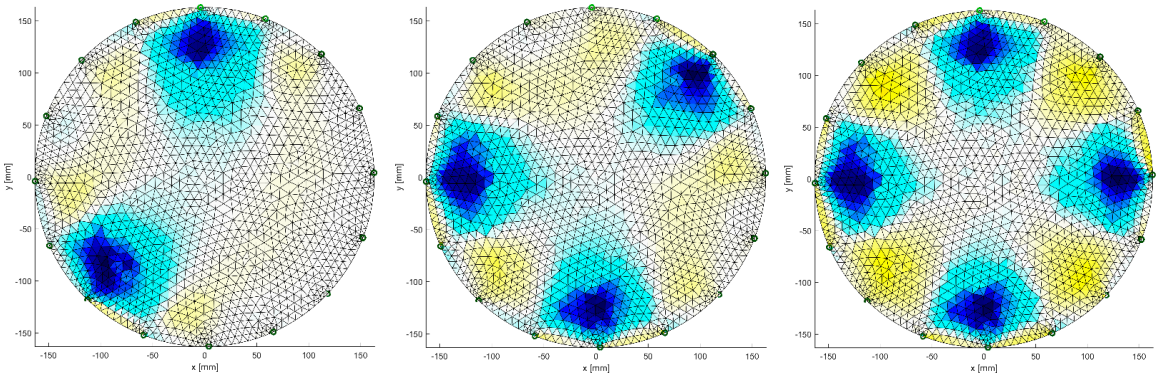

(a) (b) (c)

Figure 33. Image reconstruction for 16 measurement electrodes by Gauss-Newton method with Tikhonov regularization: (a) 2 objects, (b) 3 objects, (c) 4 objects

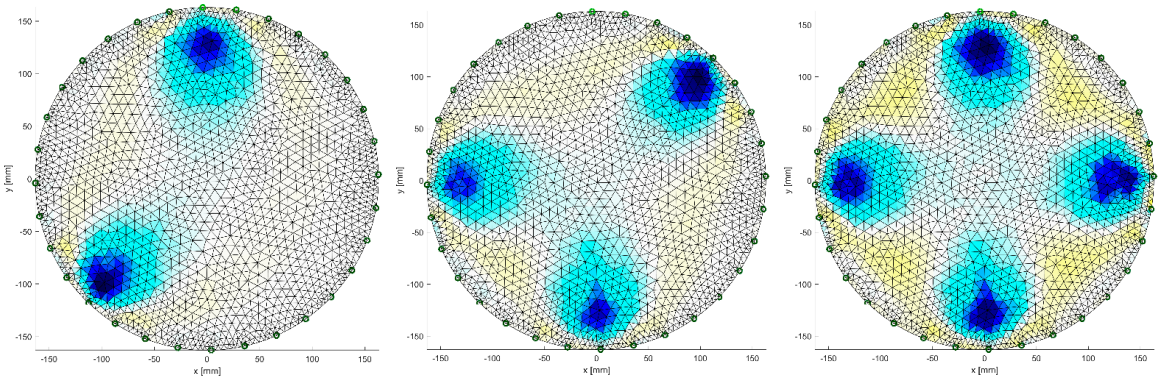

(a) (b) (c)

Figure 34. Image reconstruction for 32 measurement electrodes by Gauss-Newton method with Tikhonov regularization: (a) 2 objects, (b) 3 objects, (c) 4 objects

3.1.2. Total Variaton method

Image reconstruction using the Total Variation method for a system with 16 measuring electrodes is shown in Fig. 35. We obtain a better reconstruction quality in Fig. 36 with 32 measuring electrodes.

Preprints (www.preprints.org) | NOT PEER-REVIEWED | Posted: 29 August 2018 doi:10.20944/preprints201808.0482.v1

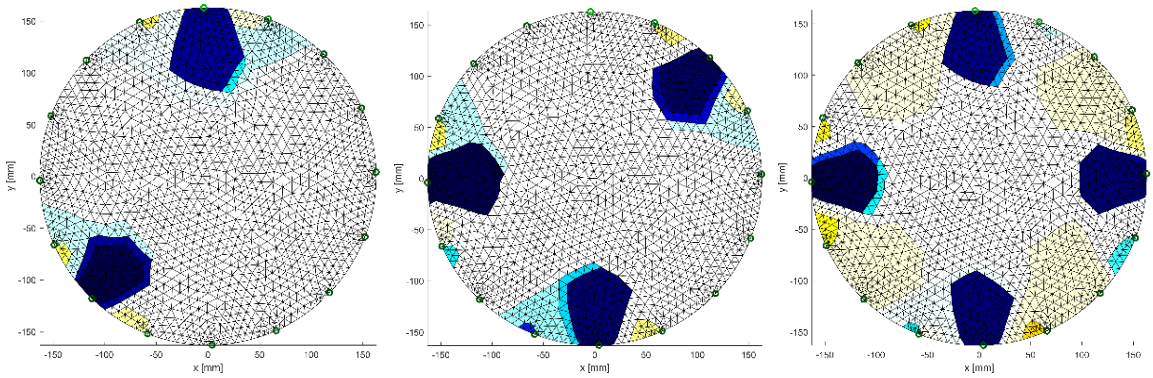

(a) (b) (c)

Figure 35. Image reconstruction for 16 measurement electrodes by Total Variation method: (a) 2 objects, (b) 3 objects, (c) 4 objects

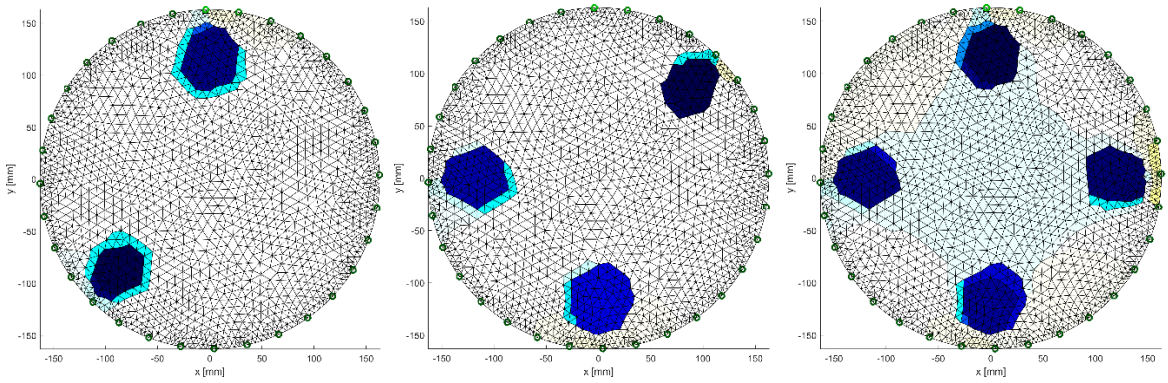

(a) (b) (c)

Figure 36. Image reconstruction for 32 measurement electrodes by Total Variation method: (a) 2 objects, (b) 3 objects, (c) 4 objects

3.1.3. Neural Networks

Image reconstruction in the case of neural networks depends largely on the training set. Therefore, reconstructions for an object with 16 electrodes (Fig. 37) gave better results than for an object with 32 electrodes (Fig. 38).

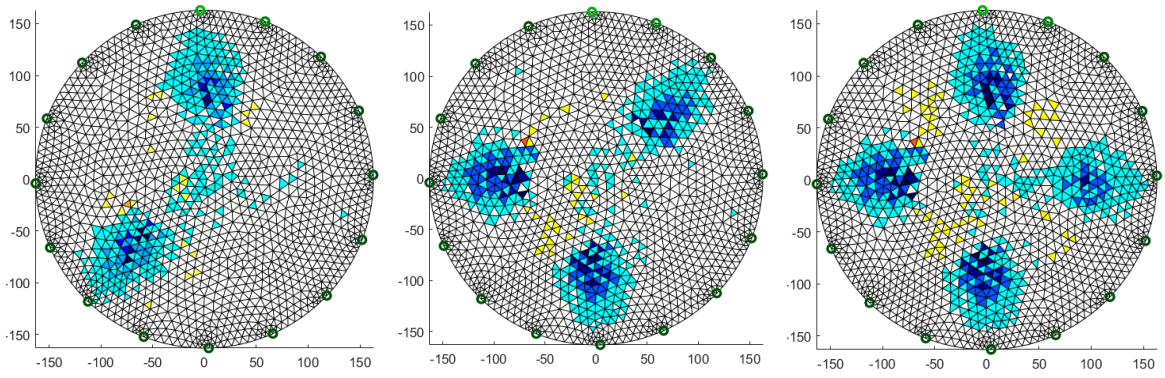

(a) (b) (c)

Figure 37. Image reconstruction for 16 measurement electrodes by Neural Networks: (a) 2 objects, (b) 3 objects, (c) 4 objects

Preprints (www.preprints.org) | NOT PEER-REVIEWED | Posted: 29 August 2018 doi:10.20944/preprints201808.0482.v1

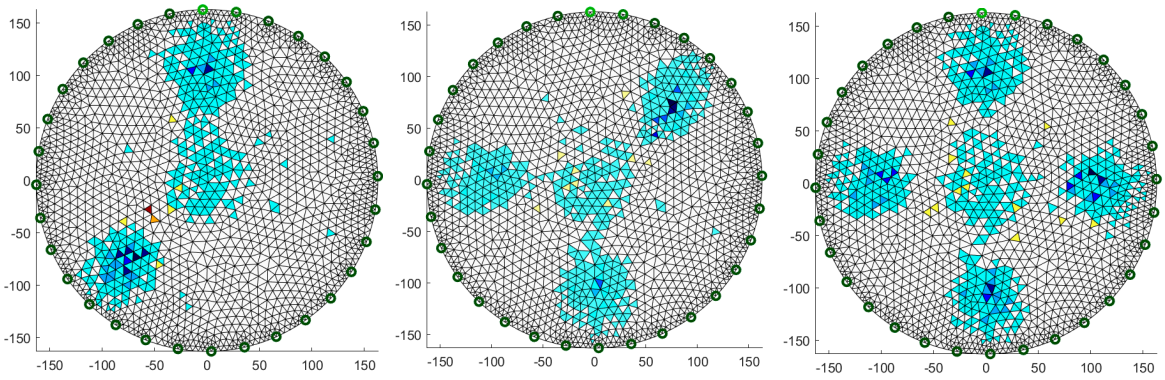

(a) (b) (c)

Figure 38. Image reconstruction for 32 measurement electrodes by Neural Networks: (a) 2 objects, (b) 3 objects, (c) 4 objects

3.1.4. Lars

Another algorithm was based on the Lars method. A teaching set of 5000 elements was used here only. In this case, the obtained results for a system with 16 electrodes (Fig. 39) are slightly worse than for a system with 32 electrodes (Fig. 40). The key element in this method is the separation of a group of independent measurements.

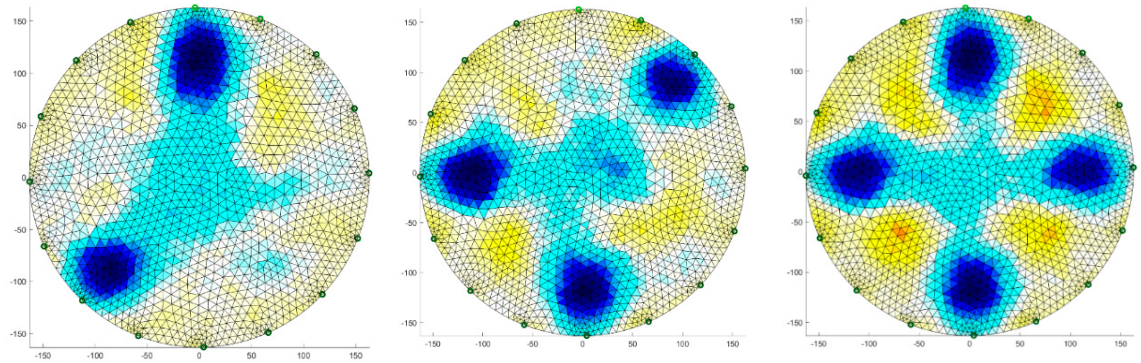

(a) (b) (c)

Figure 39. Image reconstruction for 16 measurement electrodes by Lars: (a) 2 objects, (b) 3 objects, (c) 4 objects

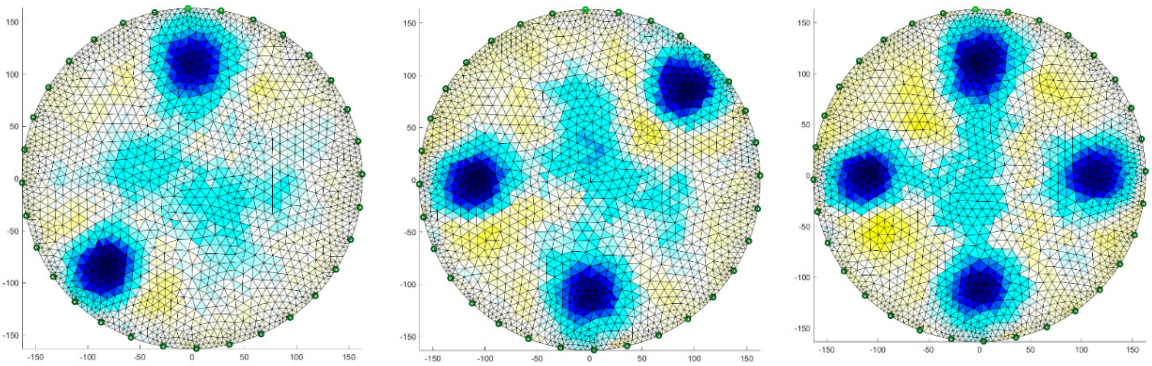

(a) (b) (c)

Figure 40. Image reconstruction for 32 measurement electrodes by Lars: (a) 2 objects, (b) 3 objects, (c) 4 objects

Preprints (www.preprints.org) | NOT PEER-REVIEWED | Posted: 29 August 2018 doi:10.20944/preprints201808.0482.v1

652 *3.1.5. Elastic net*

653 The final algorithm is Elastic net, it is more universal due to its character and gives quite precise
654 results. The same teaching set was used as for the previous method. Reconstructions for systems with
655 16 and 32 electrodes are shown in Fig. 41 and Fig. 42, respectively.
656

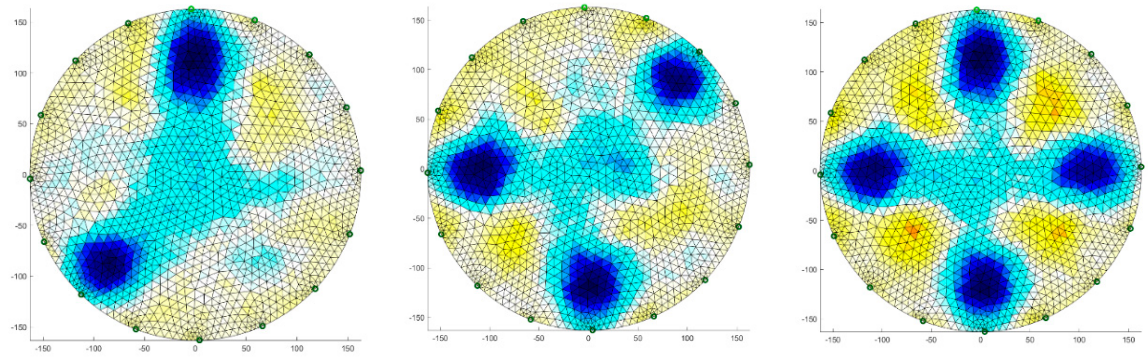

657
658 (a) (b) (c)

659 **Figure 41.** Image reconstruction for 16 measurement electrodes by Elastic net: (a) 2 objects, (b) 3 objects, (c)
660 4 objects

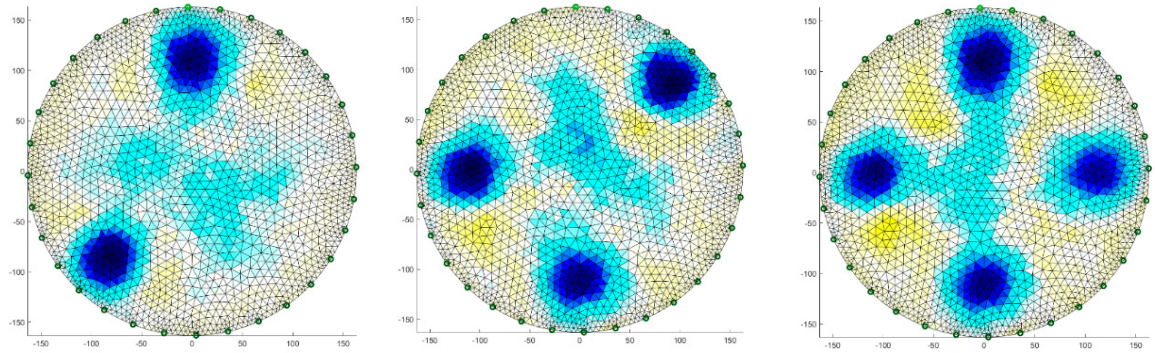

661
662 (a) (b) (c)

663 **Figure 42.** Image reconstruction for 32 measurement electrodes by Elastic net: (a) 2 objects, (b) 3 objects, (c)
664 4 objects

665 *3.1.6. Comparison of image reconstruction*

666 The summary of the presented image reconstructions for the indicated methods (Gauss-Newton,
667 Total Variation, Neural Networks, Lars and Elastic net) with 4 unknown objects for the measurement
668 system with 16 electrodes is Figure 43
669

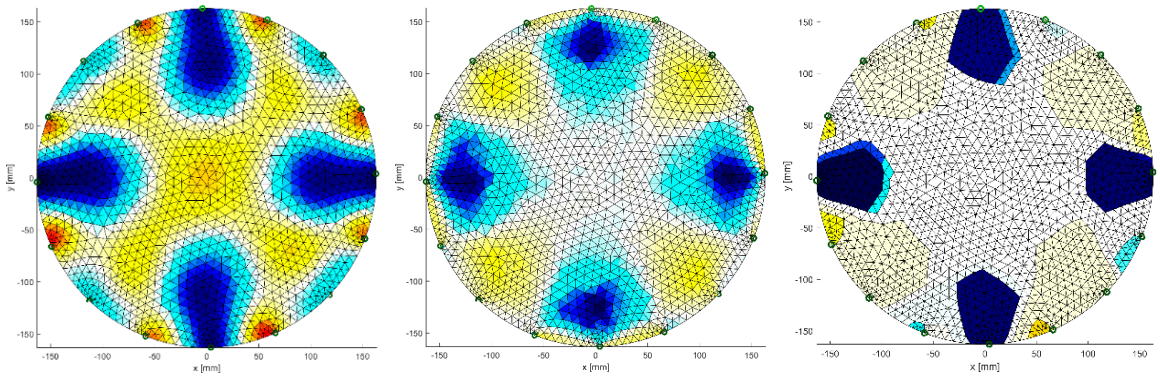

670
671 (a) (b) (c)

Preprints (www.preprints.org) | NOT PEER-REVIEWED | Posted: 29 August 2018 doi:10.20944/preprints201808.0482.v1

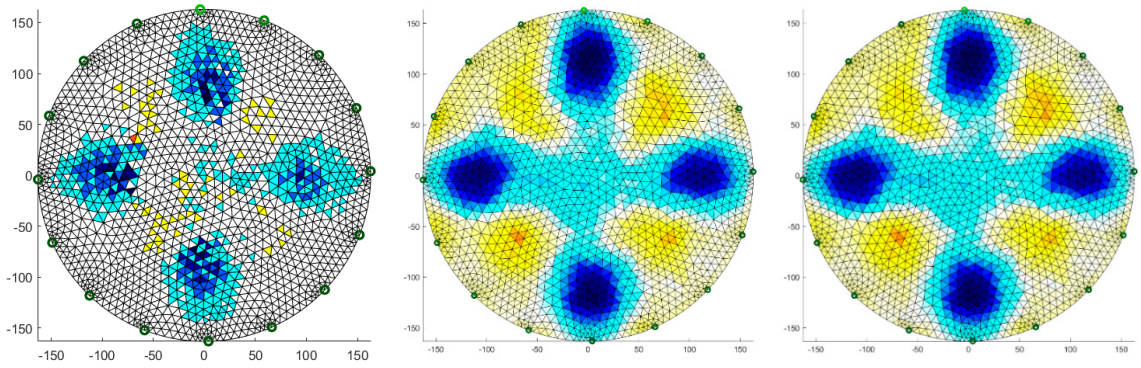

(d) (e) (f)

Figure 43. Summary of image reconstruction for different methods with 4 unknown objects- measuring system with 16 electrodes: (a) Gauss-Newton with Laplace regularization, (b) Gauss-Newton with Tikhonov regularization, (c) Total Variation, (d) Neural Networks, (e) Lars, (f) Elastic net

3.2. Image reconstruction for small objects

The analysis of processes in which there are a large number of smaller objects is of great importance in the tomography. For this purpose, individual methods have been analysed on several examples. Figure 44 presents the image reconstruction by using the deterministic method in EIT model. Reconstruction using the Lars method in ECT is shown in Figure 45. In contrast, the elastic net method was implemented for the EIT model in Figure 46. Also, for the EIT method reconstruction was performed using multiply Neural Networks (Fig. 47). Figure 48 shows a comparison of reconstructions for EIT and ECT using the elastic net method.

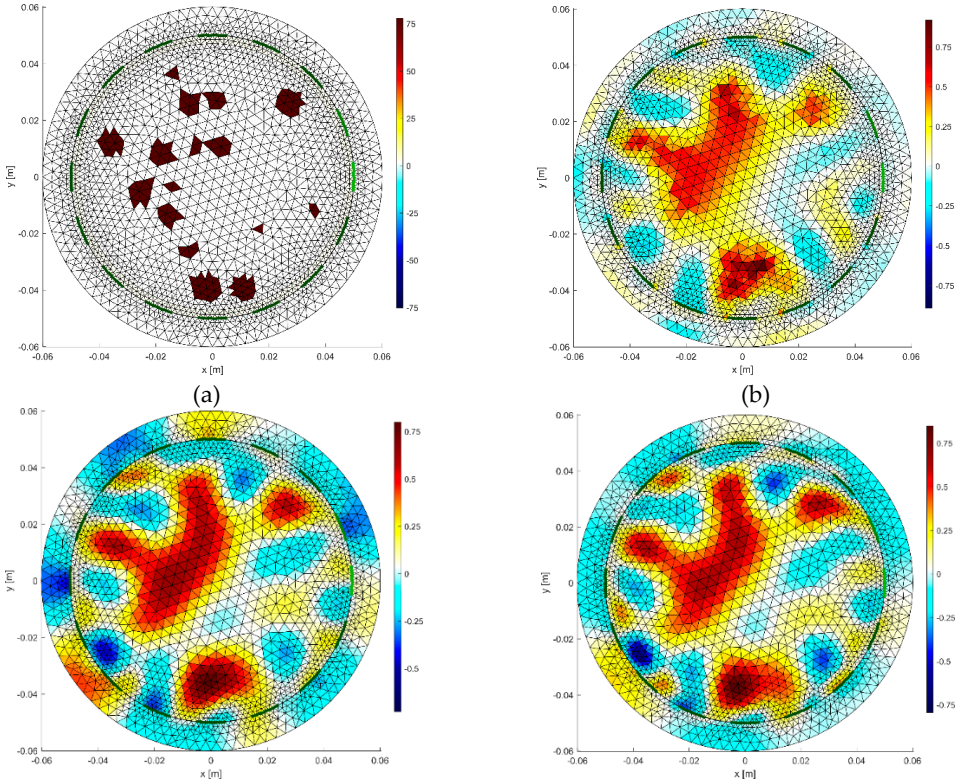

(a) (b)

(a) (b)

Figure 44. Image reconstruction - EIT model: (a) pattern, (b) Gauss-Newton method with Tikhonov regularization, (c) Gauss-Newton method with Laplace regularization, (d) Total Variation

Preprints (www.preprints.org) | NOT PEER-REVIEWED | Posted: 29 August 2018 doi:10.20944/preprints201808.0482.v1

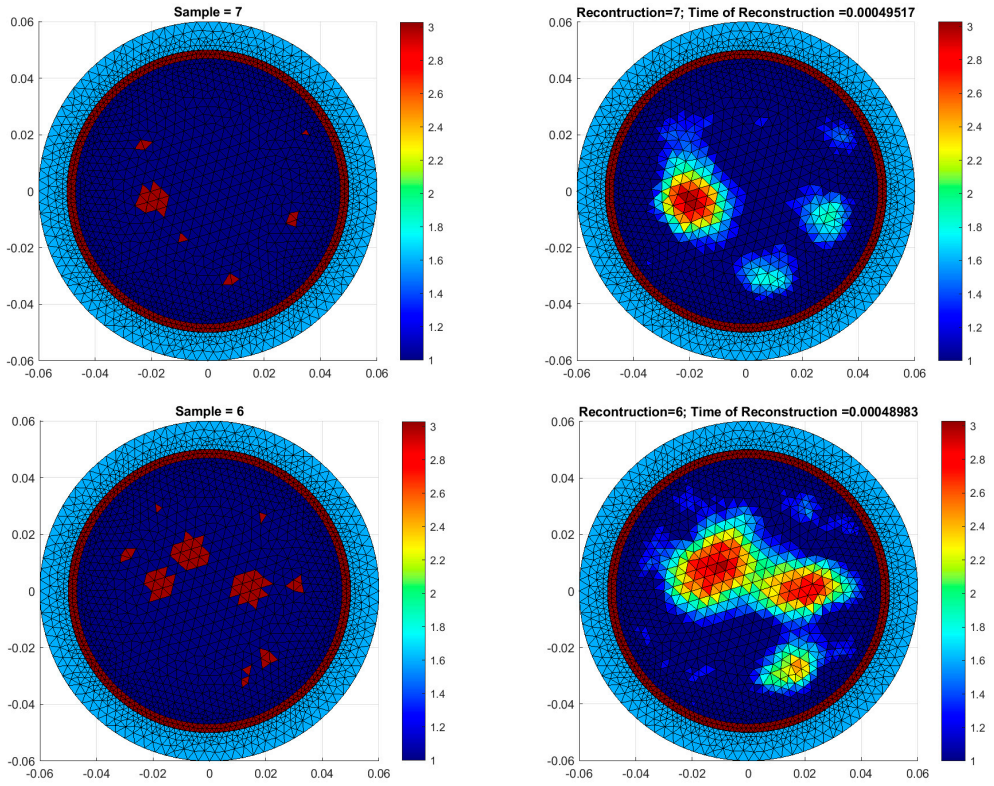

(a) (b)

Figure 45. Image reconstruction – ECT model: (a) pattern, (b) Lars

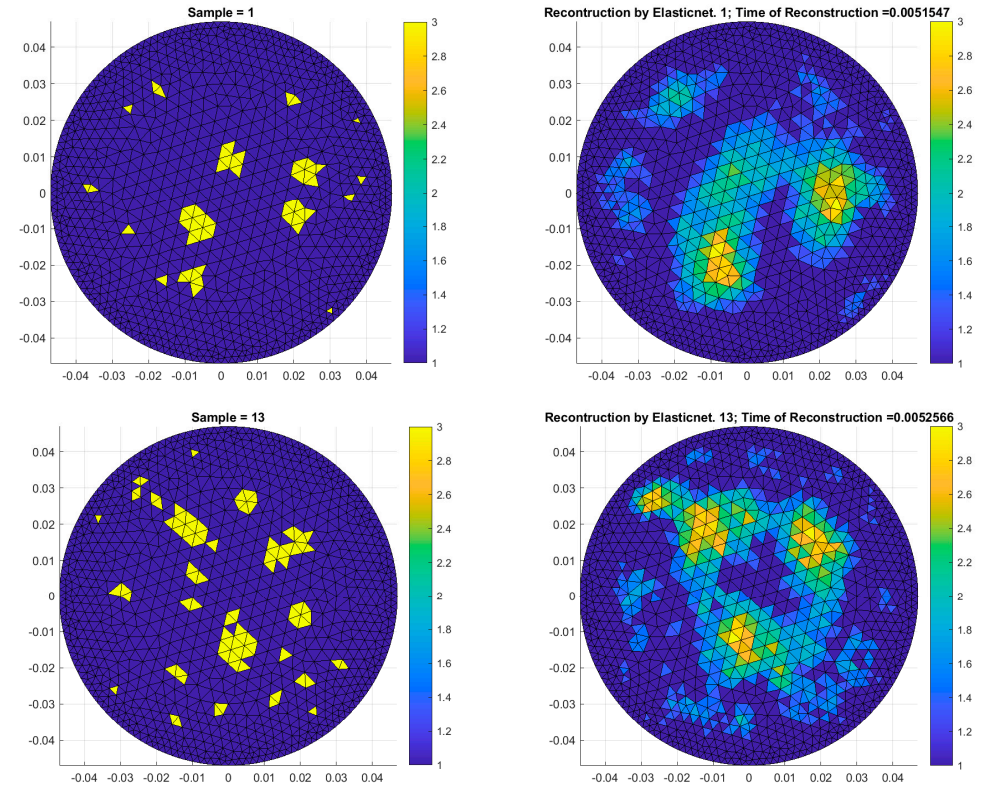

(a) (b)

Figure 46. Image reconstruction – EIT model: (a) pattern, (b)Elastic net

Preprints (www.preprints.org) | NOT PEER-REVIEWED | Posted: 29 August 2018 doi:10.20944/preprints201808.0482.v1

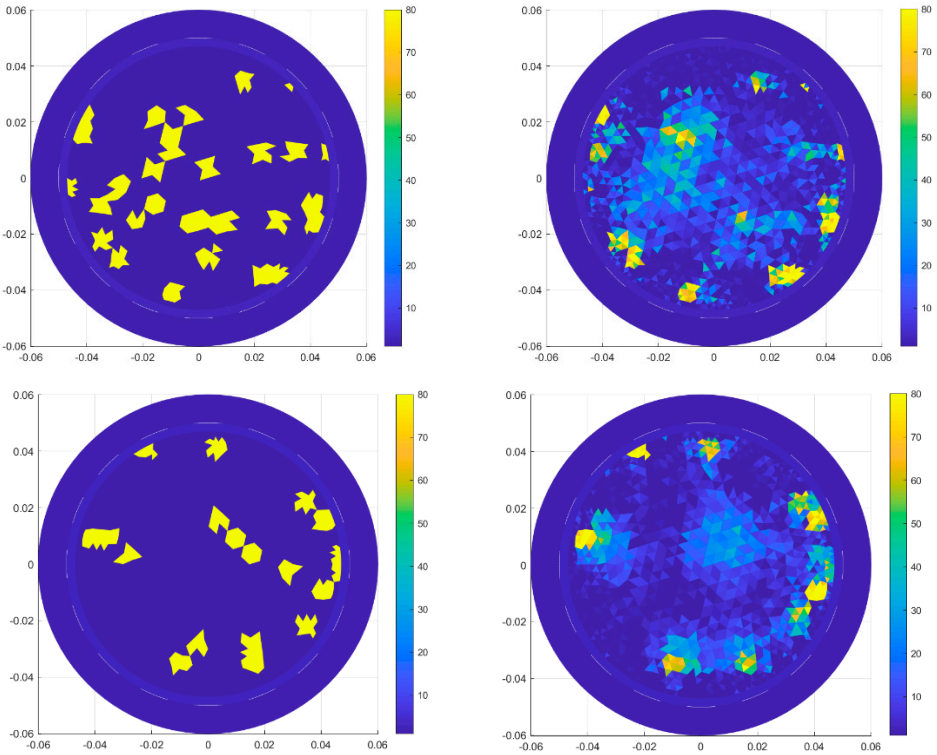

(a) (b)

Figure 47. Image reconstruction – EIT model: (a) pattern, (b) multiply Neural Network

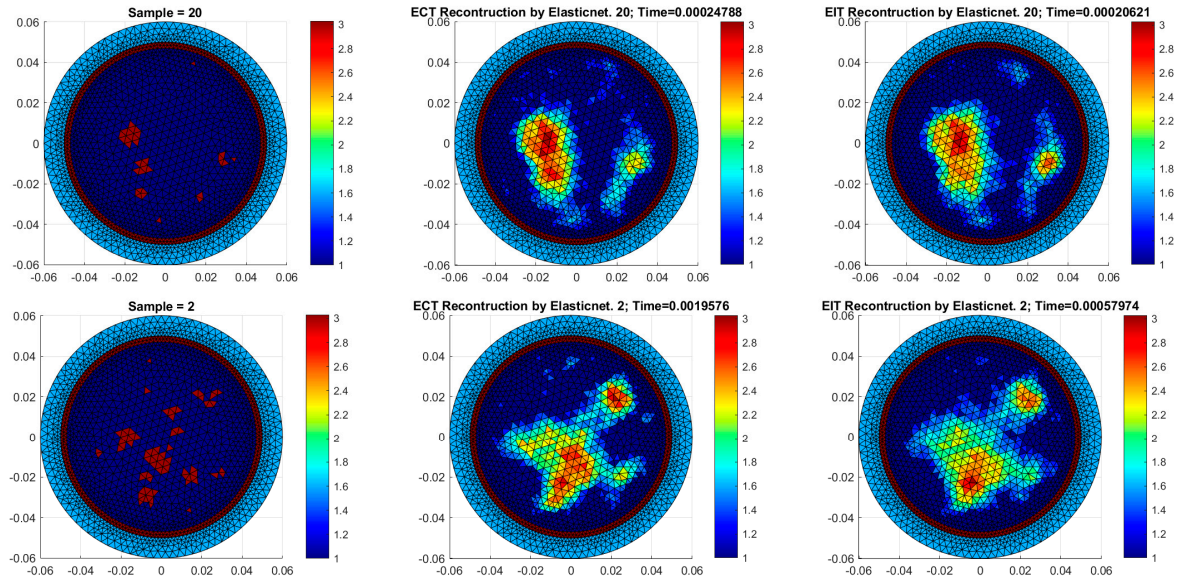

(a) (b) (c)

Figure 48. Image reconstruction by Elastic net: (a) pattern, (b) ECT, (c) EIT

3.3. Hybrid EIT/ECT

In order to improve the quality of reconstructed images, this chapter uses a hybrid combination of measurement data from the EIT and ECT methods. Figure 49 presents the results using the elastic net method, while Figure 50 shows reconstruction using the multiply Neural Network. A larger amount of input data has improved the quality of image reconstruction, especially after the use of multiply Neural Network.

Preprints (www.preprints.org) | NOT PEER-REVIEWED | Posted: 29 August 2018 doi:10.20944/preprints201808.0482.v1

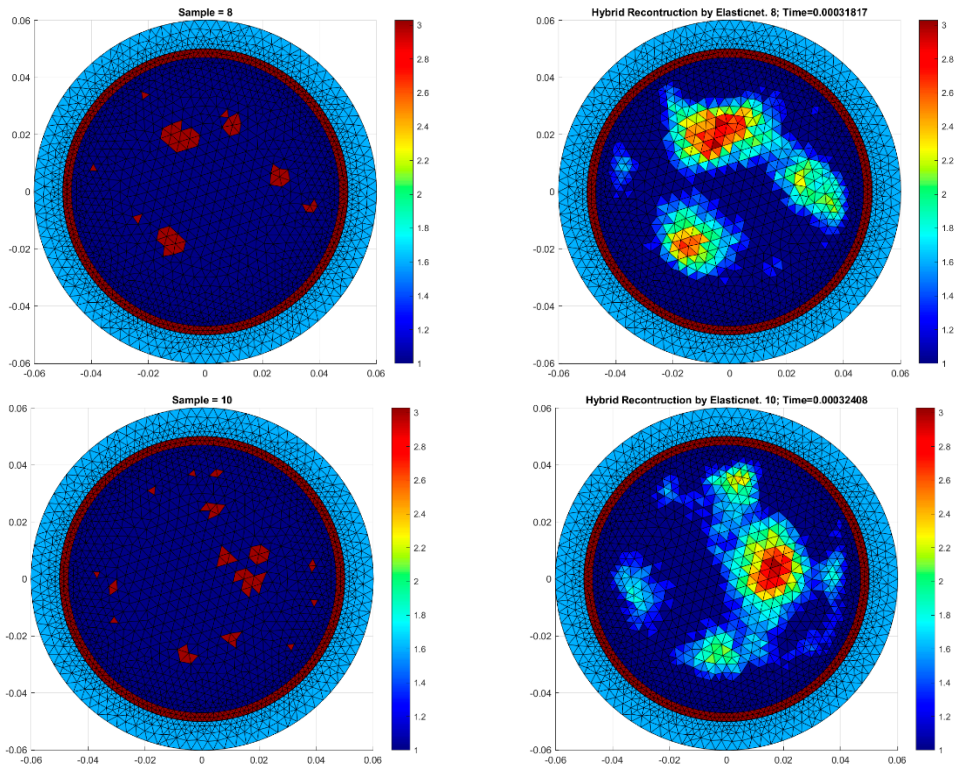

(a) (b)

Figure 49. Image reconstruction – hybrid model: (a) pattern, (b) Elastic net

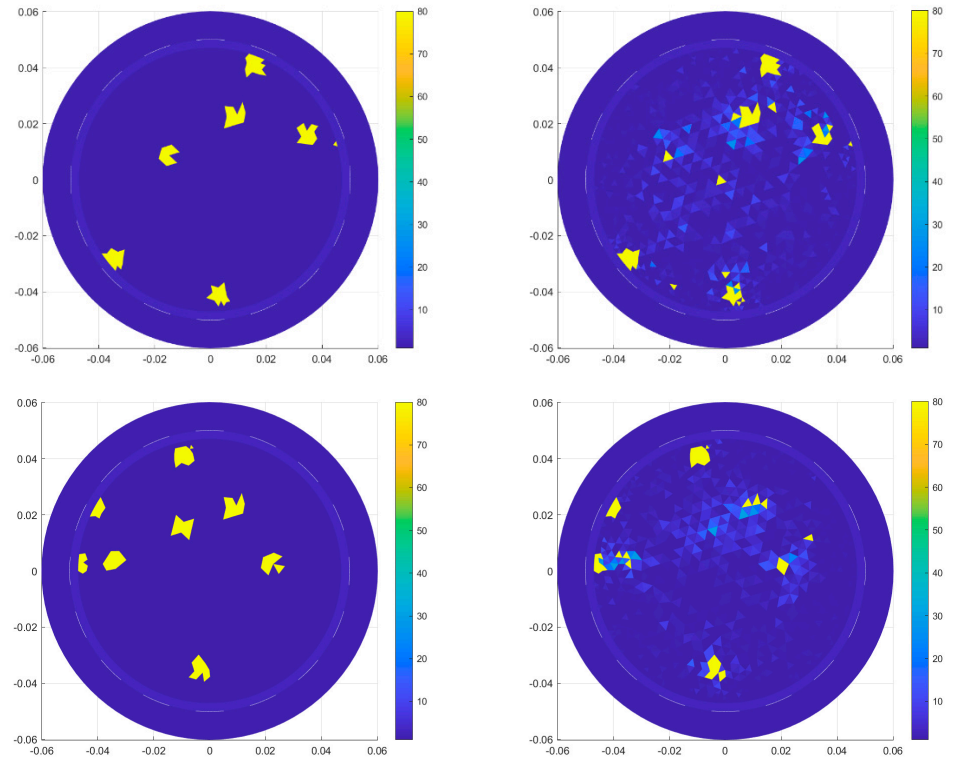

(a) (b)

Figure 50. Image reconstruction – hybrid model: (a) pattern, (b) multiply Neural Network

Preprints (www.preprints.org) | NOT PEER-REVIEWED | Posted: 29 August 2018 doi:10.20944/preprints201808.0482.v1

3.4. Image reconstruction by laboratory measurements

Figures 51-56 present the results of reconstruction of images based on laboratory measurements of the examined objects. The measuring models are described in section 2.8. A system with 16 electrodes was used here. Deterministic methods effectively reconstruct the image based on real measurements. The results obtained using neural networks depend to a large extent on the training set, therefore the quality of reconstruction is not ideal. The Lars method is quite sensitive, while Elastic net is quite universal, because by selecting the appropriate regularization parameters you can get enough good reconstructions on the actual data.

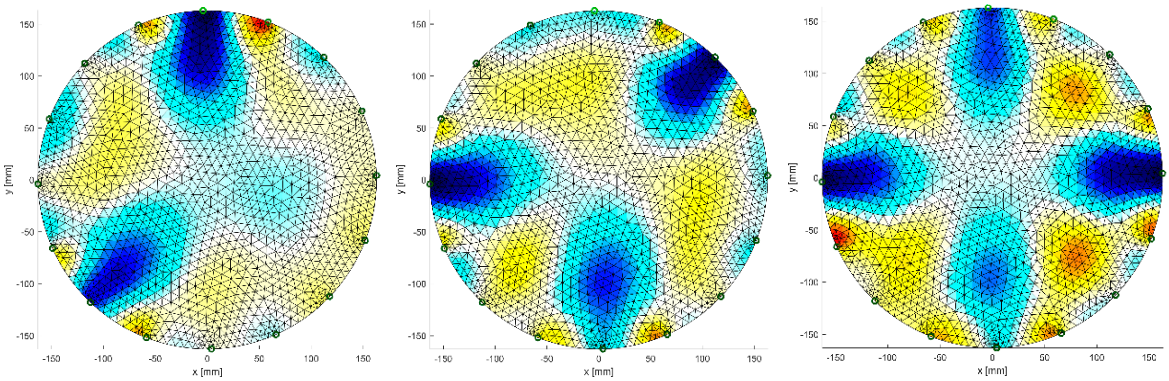

(a) (b) (c)

Figure 51. Reconstruction of images based on real measurements by Gauss-Newton method with Laplace regularization: (a) 2 objects, (b) 3 objects, (c) 4 objects

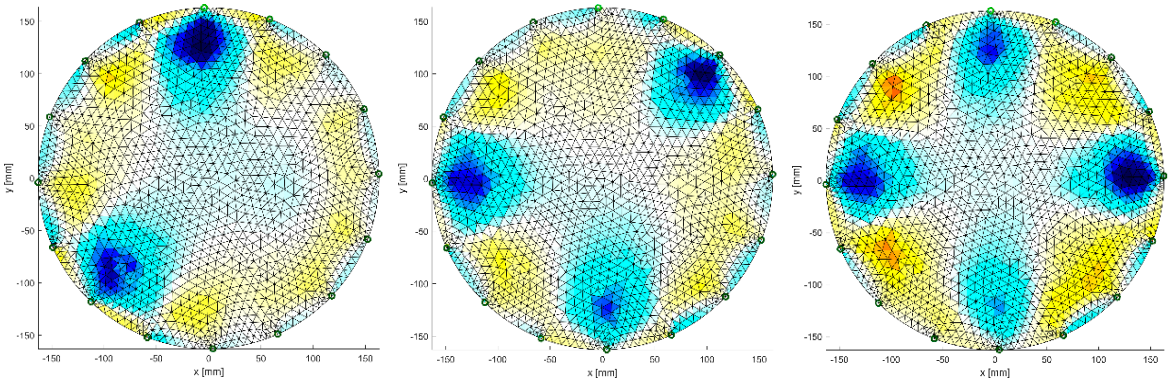

(a) (b) (c)

Figure 52. Reconstruction of images based on real measurements by Gauss-Newton method with Tikhonov regularization: (a) 2 objects, (b) 3 objects, (c) 4 objects

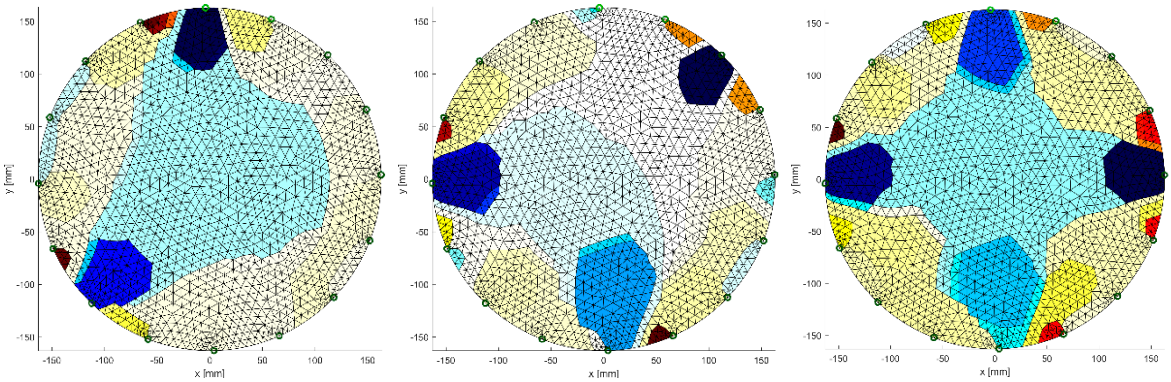

(a) (b) (c)

Figure 53. Reconstruction of images based on real measurements by Total Variation: (a) 2 objects, (b) 3 objects, (c) 4 objects

Preprints (www.preprints.org) | NOT PEER-REVIEWED | Posted: 29 August 2018 doi:10.20944/preprints201808.0482.v1

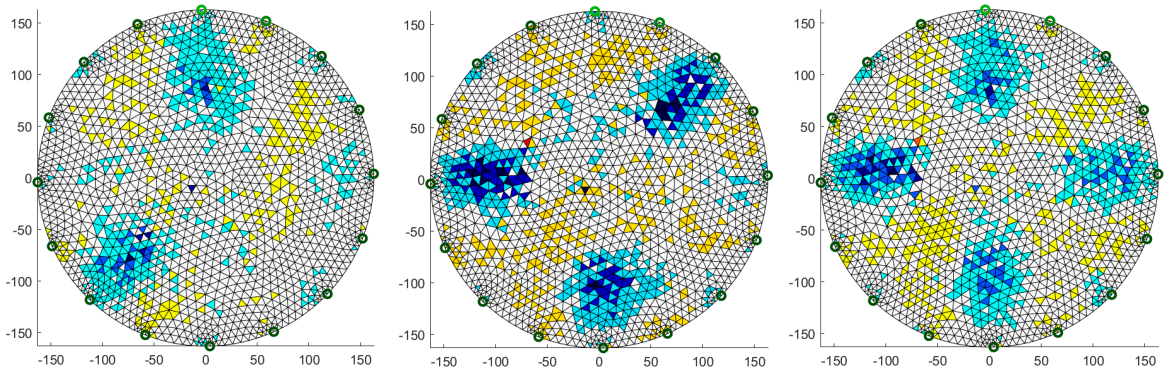

(a) (b) (c)

Figure 54. Reconstruction of images based on real measurements by Neural Network: (a) 2 objects, (b) 3 objects, (c) 4 objects

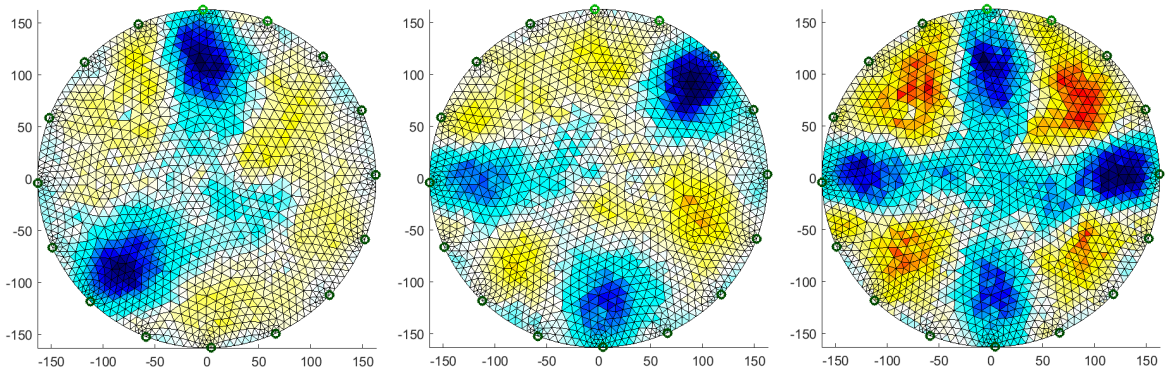

(a) (b) (c)

Figure 55. Reconstruction of images based on real measurements by Lars: (a) 2 objects, (b) 3 objects, (c) 4 objects

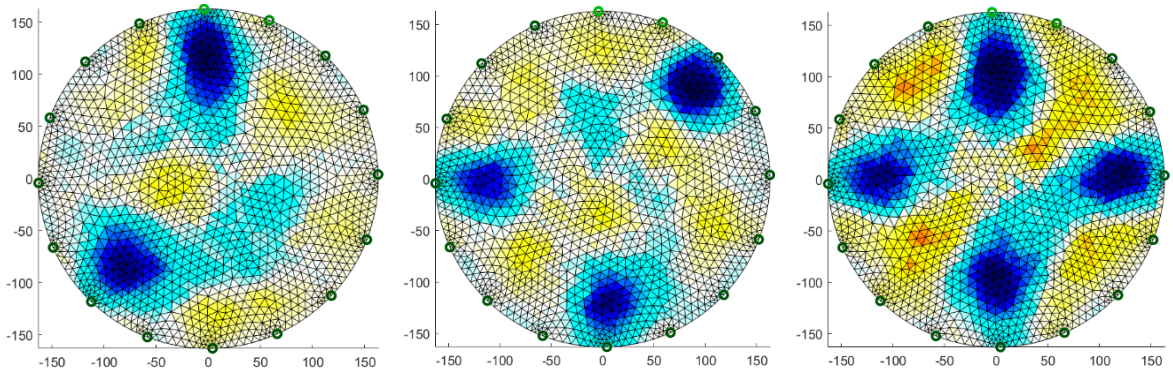

(a) (b) (c)

Figure 56. Reconstruction of images based on real measurements by Elastic net: (a) 2 objects, (b) 3 objects, (c) 4 objects

4. Discussion

4.1. Distributed tomography system

Research work presents the original concept of a complex system based on smart tomographic sensors, a cyber-physical system for process analysis in Industry 4.0. The results of the research present the use of tomographic sensors for the analysis of industrial processes using dedicated measuring devices and image reconstruction algorithms. The presented system architecture will increase the level of reliability and efficiency of technological processes in the enterprise. It will enable forecasting changes based on real-time data analysis and historical data. The communication

platform enables the management of data stored on the server, is responsible for communication of interfaces exchanging data with internal and external systems, optimizes the mechanisms of automatic control of data processing elements obtained from various tomographic sensors located in the key nodes of the installation.

4.2. Technological challenges

The presented monitoring system is aimed at automation, analysis and optimization of technological processes using industrial tomography, which allows analysis of processes taking place in the facility without interfering with its interior. This solution enables better understanding and monitoring of industrial processes and facilitates process control in real time. To design the system, an electrical tomography was used, with which technological processes are studied. The collected information is processed by an algorithm that reconstructs the image. This type of tomography is characterized by a relatively low image resolution. Difficulties in obtaining high resolution result mainly from a limited number of measurements, non-linear current flow through a given medium and too low sensitivity of measured voltages depending on changes in conductivity in the area. The main challenge in this area was to construct precise measuring devices and algorithms for image reconstruction. Other elements of the system are measurement methods using information contained in the ultrasonic signal after passing through the tested medium and wire mesh sensors, flow imaging devices and enabling testing of multi-phase flows with high spatial and temporal resolution. The idea of the measurement system was based on tomographic sensors to collect and collect data, and through appropriate communication protocols for processing in a computing cloud. The constructions of measuring devices are also an innovative solution. The design of the device with hybrid tomography is based on the simultaneous measurement of ECT and EIT. It provides a non-invasive method of testing the spatial distribution of two types of material coefficients. The ultrasonic tomograph consists of active measuring probes controlled by an external module via a CAN bus. Active measuring probes have been divided into digital and analog parts.

4.3. Image reconstruction

Data analysis is an important part of the diagnosis of the process based on tomography. Industrial tomography should be the problems of the inverse electromagnetic field. The inverse problem is the process of optimization, identification or synthesis, in which the parameters describing the field are determined based on the possession of information relevant to this field. Such problems are difficult to analyse. They do not have unambiguous solutions and are misunderstood due to too little or too much information. Knowledge of the process can make image reconstruction more resistant to incomplete information. In the article, the authors chose deterministic methods based on Gauss-Newton and Total Variation methods and machine learning methods. The Gauss-Newton method in two variants was used for image reconstruction with Laplace regularization and Tikhonov regularization. Reconstruction of the image with the use of the Total Variation method gave a better reconstruction quality in the system of 32 measuring electrodes. Reconstruction of the image in the case of neural networks depended largely on the training set. Another algorithm, based on the Lars method, had a teaching set of 5000 elements. In this case, the obtained results for a system with 16 electrodes are slightly worse than for a system with 32 electrodes. Elastic net, is more universal of the presented methods due to its character and gives quite precise results. The same teaching set was used as the Lars method. Models with a large number of smaller objects for the EIT and ECT methods were also analysed. For this purpose, individual methods have been analysed on several examples. In order to improve the image reconstruction quality, a hybrid model was also used, supplying the machine learning algorithms with EIT / ECT data simultaneously. A larger amount of input data has improved the quality of image reconstruction, especially after the use of multiply Neural Network. The final part of the research was laboratory measurements on the basis of which the image reconstruction was made. A system with 16 electrodes was used here. Deterministic methods successfully reconstructed the image. The results obtained using neural networks were worse, largely

due to the small training set. Lars and Elastic, on the other hand, proved to be quite effective in solving the problem under investigation.

4.4. Limitations and future work

In the process tomography based on electrical tomography, there is no ideal method for reconstructing and analysing data. Methods and models need to be properly selected depending on the problem that needs to be solved. Deterministic methods have a bigger problem with more reconstructed objects. Neural networks give worse results, but this is partly dependent on the training set. However, with a large training set, especially for more small objects, they are quite effective. Machine learning methods based on Lars, especially Elastic net, seem to be the most accurate, especially for real measurement data.

Further works will be focused on improving the methods of image reconstruction using deep learning and the development of measuring devices for both electrical tomography and ultrasound tomography.

5. Conclusions

The main goal of this work was to prepare an innovative application based on process tomography, a cyber-physical system and dedicated measuring devices and sensors. The research work was focused mainly on the development of measurement methods and models for the analysis and reconstruction of data using electrical tomography. Gauss-Newton with Laplace regularization, Gauss-Newton with Tikhonov regularization, Total Variation, Neural Networks, Lars and Elastic net methods were used to solve the inverse problem. The results of reconstruction of individual algorithms with different measurement models were compared. The tests were carried out for synthetic data and laboratory measurements. The system includes a communication interface, unique optimization algorithms and data analysis algorithms for image reconstruction and process monitoring. The constructed electronic devices for measuring the material values of the studied environment through cooperation with the rest of the system collect data from the measurement sensors. The obtained results illustrate spatial data resolution, which gives the possibility of visual analysis of the processes taking place inside the object. The proposed solution should bring benefits to various economic and industrial sectors.

Author Contributions: Tomasz Rymarczyk has developed system concepts, research methods and implementation of solutions in industrial tomography of the presented techniques in this article. Grzegorz Kłosowski has implemented the neural network method. Edward Kozłowski carried out research especially in the field of statistical methods. Paweł Tchórzewski worked on deterministic algorithms.

Acknowledgments: The authors would like to thank the authorities and employees of the Institute of Mathematics, Maria Curie-Skłodowska University, Lublin, Poland for sharing supercomputing resources.

Conflicts of Interest: The authors declare no conflict of interest.

References

1. Repta D., Sacala I., Moisescu M., Stanescu A. Towards the development of a Cyber-Intelligent Enterprise System Architecture, *19th World Congress The International Federation of Automatic Control*, Cape Town, South Africa. August 24-29, **2014**.
2. Monostori L. Cyber-physical production systems: Roots, expectations and R&D challenges, Variety Management in Manufacturing. *Proceedings of the 47th CIRP Conference on Manufacturing Systems, Procedia CIRP 17*, **2014**.
3. Qian F., Xu G., Zhang L., Dong H. Design of Hybrid NC Control System for Automatic Line, *International Journal of Hybrid Information Technology*, **2015**, vol. 8/4, pp. 185-192.
4. Bergweiler S. Intelligent Manufacturing based on Self-Monitoring Cyber-Physical Systems, *UBICOMM 2015 The Ninth International Conference on Mobile Ubiquitous Computing, Systems, Services and Technologies*, **2015**.

5. Wan J, Tang S., Shu Z., Li D., Wang S., Imran M, Vasilakos A. Software-Defined Industrial Internet of Things in the Context of Industry 4.0, *IEEE Sensors Journal*, vol. 16/20, **2016**, pp. 7373 – 7380.
6. Wang S., Wan J., Li D., Zhang C. Implementing Smart Factory of Industrie 4.0: An Outlook, *International Journal of Distributed Sensor Networks*, vol. 2016/7, **2016**, doi.org/10.1155/2016/3159805.
7. Zhong R., Xu X., Klotz E., Newman S. Intelligent Manufacturing in the Context of Industry 4.0: A Review, *Engineering*, vol. 3, **2017**, pp. 616–630.
8. Beck M., Williams R. Process tomography: a European innovation and its applications, *Meas. Sci. Technol.* , vol. 7, **1996**, pp. 215–224.
9. Vejar A., Cieplak T., Rymarczyk T. Cloud Computing System for online processing of ERT Data Streams, *International Interdisciplinary PhD Workshop 2018, IIPhDW 2018*, 09 - 12 May **2018**, Świnoujście, Poland.
10. Filipowicz, S.F.; Rymarczyk, T. Measurement methods and image reconstruction in electrical impedance tomography. *Przeglad Elektrotechniczny*, **2012**, vol. 88, pp. 247–250.
11. Holder D. Introduction to biomedical electrical impedance tomography Electrical Impedance Tomography Methods, History and Applications", *Bristol, Institute of Physics*, **2005**.
12. Karhunen, K.; Seppänen, A.; Kaipio, J. P. Adaptive meshing approach to identification of cracks with electrical impedance tomography, *Inverse Problems & Imaging*, **2014**, vol. 8/1, pp.127-148, doi: 10.3934/ipi.2014.8.127.
13. Rymarczyk, T.; Adamkiewicz, P.; Duda, K.; Szumowski, J.; Sikora, J. New electrical tomographic method to determine dampness in historical buildings, *Archives of Electrical Engineering*, **2016**, vol. 65, pp. 273–283.
14. AL Hosani E, Soleimani M. Multiphase permittivity imaging using absolute value electrical capacitance tomography data and a level set algorithm, *Phil. Trans. R. Soc. A*, **2016**, 374 20150332; DOI: 10.1098/rsta.2015.0332.
15. Kryszyn J., Wanta D., Smolik W. Gain Adjustment for Signal-to-Noise Ratio Improvement in Electrical Capacitance Tomography System EVT4, *IEEE Sensors Journal*, vol. 17/24, **2017**, pp. 8107-8116.
16. Majchrowicz M., Kapusta P., Jackowska-Strumiłło L., Sankowski D. Acceleration of image reconstruction process in the electrical capacitance tomography 3d in heterogeneous, multi-gpu system, *Informatyka, Automatyka, Pomiary w Gospodarce i Ochronie Środowiska (IAPGOŚ)*, **2017**, vol. 7/1, pp. 37-41; DOI: 10.5604/01.3001.0010.4579.
17. Banasiak R., Wajman R., Jaworski T., Fiderek P., Fidos H., Nowakowski J. Study on two-phase flow regime visualization and identification using 3D electrical capacitance tomography and fuzzy-logic classification, *International Journal of Multiphase Flow*, **2014**, vol. 58, pp. 1-14.
18. Garbaa H., Jackowska-Strumiłło L., Grudzień K., Romanowski A. Application of electrical capacitance tomography and artificial neural networks to rapid estimation of cylindrical shape parameters of industrial flow structure, *Archives of Electrical Engineering*, **2016**, vol. 65/4, pp. 657-669.
19. Kryszyn J., Smolik W. Toolbox for 3d modelling and image reconstruction in electrical capacitance tomography, *Informatyka, Automatyka, Pomiary w Gospodarce i Ochronie Środowiska (IAPGOŚ)*, **2017**, vol. 7/1, pp. 137-145; DOI: 10.5604/01.3001.0010.4603.
20. Soleimani M., Mitchell CN, Banasiak R., Wajman R., Adler A., Four-dimensional electrical capacitance tomography imaging using experimental data, *Progress In Electromagnetics Research*, **2009**, vol. 90, pp. 171-186.
21. Ye Z.., Banasiak R., Soleimani M. Planar array 3D electrical capacitance tomography, Insight: *Non-Destructive Testing and Condition Monitoring*, vol. 55/12, **2013**, pp. 675-680.
22. Wajman R., Fiderek P., Fidos H., Sankowski D., Banasiak R., Metrological evaluation of a 3D electrical capacitance tomography measurement system for two-phase flow fraction determination, *Measurement Science and Technology*, vol. 24/6, **2013**, p. 065302.
23. Romanowski A. Big Data-Driven Contextual Processing Methods for Electrical Capacitance Tomography, *IEEE Transactions on Industrial Informatics*, **2018**, p. 1551-3203, DOI: 10.1109/TII.2018.2855200.
24. Kryszyn J., Smolik W., Toolbox for 3d modelling and image reconstruction in electrical capacitance tomography, *Informatyka, Automatyka, Pomiary w Gospodarce i Ochronie Środowiska (IAPGOŚ)* , vol. 7/1, **2017**, pp. 137-145; DOI: 10.5604/01.3001.0010.4603
25. Kapusta P., Jackowska-Strumiłło L., Sankowski D. Acceleration of image reconstruction process in the electrical capacitance tomography 3d in heterogeneous, multi-gpu system, *Informatyka, Automatyka, Pomiary w Gospodarce i Ochronie Środowiska (IAPGOŚ)*, **2017**, vol. 7/1, pp. 37-41; DOI: 10.5604/01.3001.0010.4579.

26. Kłosowski G., Rymarczyk T., Gola A. Increasing the Reliability of Flood Embankments with Neural Imaging Method, *Applied Sciences*, vol. 8/9, **2018,** p. 1457, doi: 10.3390/app8091457.
27. Demidenko, E.; Hartov, A.; Paulsen, K. Statistical estimation of Resistance/Conductance by electrical impedance tomography measurements, *IEEE Transaction on Medical Imaging*, **2004**, vol. 23/7, pp.829-838.
28. Rymarczyk T., Characterization of the shape of unknown objects by inverse numerical methods, *Przeglad Elektrotechniczny*, **2012**, vol. 88/7B, pp. 138-140.
29. Wang M. Industrial Tomography: Systems and Applications, Elsevier, **2015**.
30. Adler, A., Lionheart, W. RB. Uses and abuses of EIDORS: an extensible software base for EIT. *Physiological measurement*, **2006**, 27.5: S25.
31. Dušek J., Hladký D., Mikulka J. Electrical Impedance Tomography Methods and Algorithms Processed with a GPU, *In PIERS Proceedings*, **2017**, pp. 1710-1714.
32. Hamilton S., Siltanen S. Nonlinear inversion from partial EIT data: computational experiments, *Contemporary Mathematics*, **2014**, vol. 615, pp. 105–129.
33. Filipowicz, S.F.; Rymarczyk, T. The shape reconstruction of unknown objects for inverse problems. *Przeglad Elektrotechniczny*, **2012**, vol. 88, pp. 55–57.
34. Lechleiter, A.; Rieder, A. Newton regularizations for impedance tomography: convergence by local injectivity. *Inverse Problems*, **2008**, 24(6) 065009.
35. Voutilainen, A.; Lehikoinen, A.; Vauhkonen, M.; Kaipio, J. Three-dimensional nonstationary electrical impedance tomography with a single electrode layer, *Measurement Science and Technology*, **2010**, vol. 21, p. 035107.
36. Koulountzios P., Rymarczyk T., Soleimani M. Ultrasonic Tomography for automated material inspection in liquid masses, *9th World Congress on Industrial Process Tomography*, Bath, 2-6 September **2018**.
37. Da Silva MJ., Schleicher E., U Hampel U. Capacitance wire-mesh sensor for fast measurement of phase fraction distributions, *Measurement Science and Technology*, vol. 18/7, **2007**, pp. 2245.
38. Hoyle B. S. IPT in Industry – Application Need to Technology Design, *ISIPT 8th World Congress in Industrial Process Tomography*, Igaussu Falls, Brazil, B11, **2016**, pp. 1-7.
39. Polakowski K., Filipowicz S.F., Sikora J., Rymarczyk T. Tomography Technology Application for Workflows of Gases Monitoring in the Automotive Systems, *Przeglad Elektrotechniczny*, **2008**, vol. 84/12, pp. 227-229.
40. Babout L., Grudzień K., Wiącek J., Niedostatkiewicz M., Karpiński B., Szkodo M. Selection of material for X-ray tomography analysis and DEM simulations: comparison between granular materials of biological and non-biological origins, *Granular Matter*, **2018**, vol. 20/3, pp. 20:38.
41. Mikulka J., GPU- Accelerated Reconstruction of T2 Maps in Magnetic Resonance Imaging, *Measurement Science Review*, vol. 4, **2015**, pp. 210-218.
42. Bartušek K.; Fiala P., Mikulka J. Numerical Modeling of Magnetic Field Deformation as Related to Susceptibility Measured with an MR System, Radioengineering, **2008**, vol. 17/4, pp. 113-118.
43. Fiala P., Drexler P., Nešpor D., Szabó Z, Mikulka J., Polívka J. The Evaluation of Noise Spectroscopy Tests, *Entropy*, vol. 18/12, **2016**, pp. 1-16.
44. Bartusek K., Kubasek R., Fiala P. Determination of pre-emphasis constants for eddy current reduction, *Measurement science and technology*, **2010**, vol. 21/10, p. 105601.
45. Kłosowski G., Kozłowski E., Gola A., Integer linear programming in optimization of waste after cutting in the furniture manufacturing, *Advances in Intelligent Systems and Computing 2018;* **2018**, vol. 637, pp. 260-270.
46. Lopato P., Chady T., Sikora R., Ziolkowski S., M. Full wave numerical modelling of terahertz systems for nondestructive evaluation of dielectric structures, *COMPEL - The international journal for computation and mathematics in electrical and electronic engineering*, **2013**, vol. 32/3, pp. 736 – 749.
47. Psuj G. Multi-Sensor Data Integration Using Deep Learning for Characterization of Defects in Steel Elements, *Sensors*, vol. 18/1, **2018**, p. 292; https://doi.org/10.3390/s18010292.
48. Mazurkiewicz D. Maintenance of belt conveyors using an expert system based on fuzzy logic, *Archives of Civil and Mechanical Engineering*, **2015**; vol. 15/2, pp. 412-418.
49. Kosicka E., Kozłowski E., Mazurkiewicz D. Intelligent Systems of Forecasting the Failure of Machinery Park and Supporting Fulfilment of Orders of Spare Parts, *Intelligent Systems in Production Engineering and Maintenance – ISPEM 2017*, **2018**, pp. 54–63.
50. Othman, M.F.; Shazali, K. Wireless sensor network applications: A study in environment monitoring system, *Procedia Engineering*, **2012**, vol. 41, pp. 1204–1210.

51. Ziolkowski M., Gratkowski S., Zywica A. R., Analytical and numerical models of the magnetoacoustic tomography with magnetic induction, *COMPEL - The international journal for computation and mathematics in electrical and electronic engineering*, **2018**, vol. 37/2, pp. 538–548.
52. Rymarczyk T., Kłosowski G., Kozłowski E. Non-Destructive System Based on Electrical Tomography and Machine Learning to Analyze Moisture of Buildings, *Sensors*, **2018**, vol. 18/7, p. 2285.
53. Hastie, T.; Tibshirani, R.; Friedman, J. The Elements of Statistical Learning Data Mining, Inference, and Prediction, Springer, New York, **2009**.
54. Wehrens R.: Chemometrics with R. Multivariate Data Analysis in the Natural Science and Life Sciences, Springer, **2011**.
55. James, G.; Witten, D.; Hastie, T.; Tibshirani, R. *An Introduction to Statistical Learning with Applications in R*, Springer, New York, **2013**.
56. Rymarczyk, T., Kłosowski, G. Application of neural reconstruction of tomographic images in the problem of reliability of flood protection facilities. *Eksploatacja i Niezawodnosc – Maintenance and Reliability*, **2018**; vol. 20/3, pp. 425–434, http://dx.doi.org/10.17531/ein.2018.3.11.
57. Madsen K., Nielsen H., Tingleff O. Methods for non-linear least squares problems, *Informatics and Mathematical Modelling*, IMM, **2004**.
58. Farha M. Combined Algorithm of Total Variation and Gauss-Newton For Image Reconstruction In Two-Dimensional Electrical Impedance Tomography (EIT), *2017 International Seminar on Sensor, Instrumentation, Measurement and Metrology (ISSIMM)* Surabaya, Indonesia, August 25th - 26th, **2017**.
59. Estrela V. , Magalhães H., Saotome O. Total Variation Applications in Computer Vision, Handbook of Research on Emerging Perspectives in Intelligent Pattern Recognition, Analysis, and Image ProcessingChapter: Total Variation Applications in Computer Vision, **2016**, DOI: 10.4018/978-1-4666-8654-0.ch002.
60. Fonseca T., Goliatt L., Campos L., Bastos F., Barra L., Santos R. Machine Learning Approaches to Estimate Simulated Cardiac Ejection Fraction from Electrical Impedance Tomography, *IBERAMIA 2016*, LNAI 10022, **2016**, pp. 235–246.
61. McCann L., Welsch R. Robust variable selection using least angle regression and elemental set sampling, Computational Statistics & Data Analysis, vol. 52, 2007, pp. 249 – 257.
62. Efron B., Hastie T., Johnstone I., Tibshirani R. Least angle regression, *The Annals of Statistics*, vol. 32/2, **2004**, pp. 407–451.
63. Xin Yan, Xiao Gang Su: Linear regression analysis: Theory and computing, *World Sciencific*, **2009**.
64. Zou, H., Hastie, T. Regularization and variable selection via the elastic net. *Journal of the Royal Statistical Society*, Series B, **2005**, vol./2, pp. 301–320.
65. Tibshirani, R. Regression shrinkage and selection via the lasso, Journal of the Royal Statistical Society, Series B, **1996**, vol. 58/1, pp. 267–288.
66. Lee Y., Nguyen V., Wang D., On Variable and Grouped Selections of the Elastic Net, Report CS532, **2016**, pp. 1–24.